CANADA



# THE HOT-TEARING OF COPPER ALLOYS

A. COUTURE & J. O. EDWARDS

PHYSICAL METALLURGY DIVISION

DEPARTMENT OF MINES AND TECHNICAL SURVEYS, OTTAWA

MINES BRANCH

RESEARCH REPORT

R 164

Price $1.00

JUNE 1965

Available by mail from the Queen's Printer, Ottawa,
and at the following Canadian Government bookshops:

OTTAWA
*Daly Building, Corner Mackenzie and Rideau*

TORONTO
*Mackenzie Building, 36 Adelaide St. East*

MONTREAL
*Aeterna-Vie Building, 1182 St. Catherine St. West*

or through your bookseller

A deposit copy of this publication is also available
for reference in public libraries across Canada

Price $1.00 Catalogue No. M38 -1/164

*Price subject to change without notice*

ROGER DUHAMEL, F.R.S.C.
Queen's Printer and Controller of Stationery
Ottawa, Canada
1965

Mines Branch Research Report R 164

# THE HOT-TEARING OF COPPER ALLOYS

by

A. Couture* and J. O. Edwards**

- - - - - - -

## ABSTRACT

A test and a rating method have been developed to assess the hot-tearing susceptibility of cast copper alloys. Thirteen alloys were rated, and, while the limitations of individual hot-tear tests are well known, it is considered that such a rating should serve as a general guide to enable foundrymen to select alloys with the best hot-tear resistance where this may be important in a particular casting design.

The probable process by which these alloys - particularly tin bronzes - solidify is tentatively related to the hot-tearing mechanism, which is discussed in general terms.

From this type of study, it may be possible to design alloys of improved hot-tear resistance, or to anticipate hot-tearing difficulties in new alloys designed from other considerations.

---

*Senior Scientific Officer, and **Head, Non-Ferrous Metals Section, Physical Metallurgy Division, Mines Branch, Department of Mines and Technical Surveys, Ottawa, Canada.

Direction des mines

Rapport de recherches R 164

# LA CRIQUABILITÉ À CHAUD DES ALLIAGES DE CUIVRE

par

A. Couture* et J. O. Edwards**

- - - -

## RESUME

Les auteurs ont mis au point un essai qui permet d'évaluer rapidement la criquabilité à chaud des alliages de cuivre de fonderie. Ils ont ainsi classé treize alliages et, quoiqu'étant au fait des limitations de la méthode, ils sont d'avis qu'une telle classification peut aider le fondeur à choisir les alliages qui sont les moins sujets à ce défaut, là où il pourrait se présenter dans un moulage donné.

Ils ont tenté de relier la formation des criques à chaud à la façon dont ces alliages se solidifient, particulièrement dans le cas des bronzes à l'étain.

Grâce à cette étude, il sera peut-être possible d'élaborer des alliages de cuivre ayant une plus faible criquabilité à chaud, ou encore de prévoir les problèmes qui pourront surgir dans les alliages nouveaux.

*Agent scientifique senior et **chef, Section des métaux non ferreux, Division de la métallurgie physique, Direction des mines, ministère des Mines et des Relevés techniques, Ottawa, Canada.

CONTENTS


| | Page |
|---|---|
| Abstract | i |
| Résumé | ii |
| Introduction | 1 |
| Pattern | 1 |
| Mould | 3 |
| Materials | 3 |
| Melting and Casting | 3 |
| Method of Assessing Hot-Tear Susceptibility | 4 |
| Results | 5 |
| Examination of Hot-Tear Pieces | 8 |
| Fracture Examination | 8 |
| Estimation of Temperature of Fracture | 8 |
| Metallographic Examination | 9 |
| Grain Size Determination | 11 |
| Thermal Analysis | 11 |
| Discussion | 12 |
| Previous Work | 12 |
| Comparison of Previous Work with Present Results | 15 |
| Temperature of Hot-Tearing | 17 |
| External vs Internal Hot-Tears | 17 |
| Discrepancy Between Main and Preliminary Experiments | 18 |
| Discrepancy from Melt to Melt | 18 |
| Assessment of Crack Rating Method | 19 |
| Influence of Constitution on Hot-Tearing | 20 |
| (a) Mode of Solidification of the Various Alloys | 20 |
| (b) Influence of Mode of Solidification on Hot-Tearing | 24 |
| Conclusions | 27 |
| References | 29 |
| Figures 1-31 | 32-49 |
| Tables 1-5 | 50-54 |

## FIGURES


| No. | | Page |
|---|---|---|
| 1. | Hot-tear Pattern | 32 |
| 2. | Hot-tear Casting | 33 |
| 3. | Alloy: 4A (85-5-5-5). Honeycomb appearance of hot-tear fracture | 34 |
| 4. | Alloy: 1A (88-10-0-2). Hot-tear fracture with wide and differently oriented facets | 34 |
| 5. | Alloy: 4A (85-5-5-5). Hot tensile fracture - 800°C | 34 |
| 6. | Alloy: 1A (88-10-0-2). Hot tensile fracture - 800°C | 34 |
| 7. | Alloy: 3A (80-10-10). Suggestion of lead globules alignment at the hot spot of the bar casting | 35 |
| 8. | Alloy: 3A (80-10-10). Segregation of delta phase at hot spot of bar; probably healed hot-tear | 35 |
| 9. | Alloy: B.N.F. (87.5-7.5-3-2). Healed hot-tear at hot spot of casting | 35 |
| 10. | Alloy: 1A (88-10-0-2). Partly healed hot-tear. Root of external tear seen at left of photograph | 36 |
| 11. | Alloy: 4A (85-5-5-5). Band of delta phase and holes in a direction normal to main axis of bar; ball side | 36 |
| 12. | Alloy: 1A (88-10-0-2). Heavy stringer of delta phase joining the root of an external hot-tear (top). Also a stringer of delta perpendicular to main axis of bar | 37 |
| 13. | Alloy: 1A (88-10-0-2). Concentration of delta phase in line with an external hot-tear (left). Partly healed hot-tear | 37 |
| 14. | Alloy: 6A (72-1-3-24). Concentration of delta phase at root of external crack | 38 |
| 15. | Alloy: Inco (84.5-6.5-3.5-3.5-2). Concentration of delta phase at root of crack (left). Note that delta phase is more dispersed than in other alloys | 38 |
| 16. | Alloy: 1A (88-10-0-2). Band of delta phase on bar side of fracture (top). A crack (bottom) is also lined with delta phase | 39 |
| 17. | Alloy: 5A (81-3-7-9). Very heavy concentration of delta phase on bar side of fracture | 39 |
| 18. | Alloy: 6A (72-1-3-24). Bar side of fracture shows heavy stringers of delta phase whereas average microstructure contains little delta phase | 40 |
| 19. | Alloy: B.N.F. (87.5-7.5-3-2). Very heavy concentration of delta phase at fracture edge on bar side | 40 |
| 20. | Alloy: B.N.F. (87.5-7.5-3-2). Concentration of delta phase at fracture edge on bar side. | 40 |

## FIGURES (Cont'd)


| No. | | Page |
|---|---|---|
| 21. | Alloy: 6A (72-1-3-24). Sharp peak in fracture section contains appreciably more delta phase than underlying material. | 41 |
| 22. | Alloy: 4A (85-5-5-5). Section through fracture of a bar mounted on end contains appreciably more delta phase than normal microstructure of alloy. | 41 |
| 23. | Copper-Tin Phase Diagram | 42 |
| 24. | Copper-Lead Phase Diagram | 43 |
| 25. | Copper-Zinc Phase Diagram | 44 |
| 26. | Tin-Lead Phase Diagram | 44 |
| 27. | Miscibility Gap in Copper-Tin-Lead System | 45 |
| 28. | Liquidus and Separation Surfaces of the Copper-Tin-Lead System | 46 |
| 29. | Miscibility Gap in Copper-Zinc-Lead System | 47 |
| 30. | Copper-Iron-Silicon Diagram, 2 wt % Iron Section | 48 |
| 31. | Copper-Aluminum Phase Diagram | 49 |


## TABLES


| No. | | Page |
|---|---|---|
| 1. | Chemical Composition | 50 |
| 2. | Crack Rating in Preliminary Experiment | 51 |
| 3. | Crack Rating in Main Experiment | 52 |
| 4. | Influence of Pouring Temperature on Crack Rating | 53 |
| 5. | Results of Differential Thermal Analysis | 54 |


= = =

# INTRODUCTION

Hot-tearing is defined as the formation of cracks in a casting at a temperature above the solidus, caused by the stresses developed in the casting during solidification and cooling.

Although the problem of hot-tearing is widely appreciated in both aluminum and ferrous casting alloys, it does not appear to be generally acknowledged in other materials, probably because its occurrence is not so marked. Previous work [1] has shown that magnesium alloys had various hot-tearing characteristics, and British work has indicated that certain phenomena, such as layer porosity in bronzes, are associated with hot-tearing.

In considering the type of porosity that often occurs in large bronze castings, it was thought that much of the problem of "leakers" was due to internal hot-tears, rather than to simple shrinkage phenomena, which are usually held to be responsible. For this reason, it was decided to investigate the hot-tearing characteristics of a number of copper casting alloys to determine whether, within a certain class, any alloy is markedly superior to its companions in this respect.

# PATTERN

The pattern used in this investigation is a modification of patterns developed by other investigators [2, 3, 4]. Bars of different lengths are cast from a common sprue. Each bar carries an enlarged section at one end (which provides a hot spot) and a flange at the other; these ends thus hinder the contraction of the bar after its solidification. Because the long bars contract more than the short ones, the strain imposed on the last-to-freeze section of the bar, i.e. the hot spot, is greater in the long bars than in the short ones and the long bars therefore tend to crack more readily. The purpose of the test is, thus, to measure the maximum bar length which can be cast, without cracking, for each alloy and condition investigated. Alternatively, the extent of cracking in each bar can be assessed and this used to rate the hot-tear susceptibility of the alloys.

In preliminary work, a mould consisting of four 1/2-in. diameter bars, cast respectively in lengths of 6, 10, 14 and 18 in., was used to find the approximate critical bar length for each alloy and casting condition.

The pattern was essentially similar to that shown in Figure 1, but in the first design the sprue: runner; gate: casting ratio was 1: 1.2: 0.9: 0.65 and each ball carried a 1 1/2-in. diameter open riser. With this pattern, however, the minimum pouring temperature which could be used with leaded tin bronzes was in the vicinity of 1200°C (2190°F). This was considered to be too high and led to a number of difficulties, such as excessive penetration and veining, gas pick-up, excessive loss of zinc, etc.

Consequently, the runner and gate cross-sections were enlarged in order to deliver the molten metal to the mould cavity at a faster rate; the risers were removed from the balls so that the full hydrostatic head maintained in the sprue during pouring would be operative on the metal flowing into the casting cavity; and the vents over the flanges were enlarged in order to decrease the back pressure in the mould cavity during the pouring operation. This modified pattern provided a sprue: runner: gate: casting ratio of 1: 2: 2: 0.65, and the pouring temperature could be decreased by approximately 100°C (180°F), with the result that the range of pouring temperatures investigated could cover the temperatures normally used in practice for the various alloys.

It was found that, in general, the 6-in. bar did not crack, and it was replaced by a 12-in. bar in order to increase the sensitivity of the test. Thus, the final pattern used in this investigation contains 10-, 12-, 14- and 18-in. bars as illustrated in Figure 1. A specimen of the castings obtained from it is shown in Figure 2.

As explained earlier, the 2-in. diameter ball at the sprue end of the bar restricts contraction and provides a hot spot where tears are likely to occur, such as that shown in the longest bar of Figure 2. It was found that cracking could be restricted to that zone provided the centre of the flange at the opposite end was sufficiently thin, i.e. approximately 1/4 in.; otherwise, cracks were occasionally found also at the junction of the flange and the bar. In order to ensure that the same amount of metal flows through the hot spot of all the bars, and hence that the hot spot is at the same temperature in all, the back side of the flange was built up in the 10-, 12- and 14-in. bars, as shown in Figures 1 and 2. The thickness of this build-up ring is greatest for the 10-in. bar, to compensate for the shorter bar length. The possible difference in loss of temperature caused by the relative position of the bars within the mould was ignored, since it was thought that this would not have any significant effect.

## MOULD

The hot-tear bars were cast in green sand moulds, with the exception of the back of the flange where a core was used. The moulds were made of McConnellsville sand, which is a synthetic unwashed sand to which 5% Western bentonite and 1/2% sand conditioner (proprietory product) are added. Throughout the tests, mould properties were controlled within the following limits: moisture content 4 to 5%, permeability 40 to 50, mould hardness (measured near the hot spot and the flange) 65 to 70 units (Dietert tester), and green compressive strength 4.5 to 6.5 psi.

## MATERIALS

The chemical analysis results (as determined by the Analytical Chemistry Sub-Division of the Mineral Sciences Division) on all alloys investigated are listed in Table 1, together with the composition ranges specified by ASTM Standards*, where applicable. For most alloys the first melt was prepared from commercial ingots. In other cases, ingots from a standard alloy were used to which additions of pure metal were made in order to bring the level of each element in the charge to the required composition. When additional melts were prepared, the scrap from previous melts of the same alloy was used, together with the additions required to keep the metal composition within the limits imposed by specifications. However, occasionally through the series a melt was made entirely from virgin metal in order to decrease the possibility of contamination.

## MELTING AND CASTING

Charges of 140 to 200 lb were melted in a lift-coil induction furnace, without using any cover, and degassed with nitrogen at a flow rate of 5 litres per min for 15 to 20 min. Most additions were made at a temperature of 1150°C (2100°F) before the degassing operation; however, zinc was added after the degassing treatment, in order to minimize zinc losses. Copper-15% phosphorus master alloy was vigorously stirred into the bronze melts approximately 1 to 2 min before pouring.

* ASTM Standards were used because of the wide acceptance of the alloy nomenclature. Corresponding CSA specifications are to be found in CSA Standards HC. 3-1962, Copper Alloy Ingots for Remelting, and HC. 9-1962, Copper Alloy Sand Castings.

In preliminary experiments, four moulds were cast from each melt at each of the following temperatures: 1275°C, 1250°C, 1225°C, and 1200°C (2325°F, 2280°F, 2235°F, and 2190°F), as shown in Table 2. In the main experiment, which could be carried out at lower temperatures on account of the pattern alterations previously described, the casting temperatures were arbitrarily established at approximately 200, 150 and 100°C (360, 270 and 180°F) above the estimated liquidus of the alloy and were as shown in Table 3.

## METHOD OF ASSESSING HOT-TEARING SUSCEPTIBILITY

As mentioned earlier, the original intention was to determine the maximum bar length which could be cast, without cracking, for each alloy and pouring condition. After a few tests, it became evident that the method was impractical since the hot-tearing susceptibility of copper alloys varies greatly; e.g., the 18-in. bars did not show any crack in some alloys, whereas even the 6-in. bars of other alloys exhibited extensive cracking. The maximum bar length method was abandoned, therefore, in favour of a rating method which made it possible to use the same pattern for all the alloys.

This method of assessing the hot-tearing susceptibility consists of assigning to each cast bar a number which corresponds to the extent to which the bar was found to have cracked at the hot spot, i.e. at the junction of the ball with the bar (Figures 1 and 2), when examined with a 5X hand lens. The rating system used was as follows:

0 corresponds to a casting which appears crack-free,

1 corresponds to a hairline crack which extends over approximately 1/2 the circumference of the bar,

2 corresponds to a hairline crack which extends over the entire circumference of the bar,

3 corresponds to a wide crack which extends over the entire circumference of the bar, and

4 corresponds to a completely fractured bar.

The 0 and 4 levels were, of course, easy to determine, but the intermediate levels 1, 2 and 3 were more difficult. In order to help the observers, two typical specimens corresponding to these intermediate levels were selected by the observers and set aside to be used as comparison standards. All the cracked bars were then compared with these standards and each bar was given the number or fraction that represented the crack under examination. The numbers so obtained were then added and the totals were considered to represent the hot-tearing susceptibility of the alloy under the particular conditions of the experiment. Cracks were assessed by at least two observers and the results were sufficiently close to present only the average in this report. Experience showed that this method was more sensitive, and more amenable to mathematical treatment, than that of measuring only the maximum uncracked bar length.

## RESULTS

The crack rating results from the preliminary experiment are given in Table 2, and those for the main experiment in Table 3. In Table 4 the hot-tearing susceptibility of the alloys studied at each pouring temperature is reported as a percentage of the susceptibility of leaded red brass (4A alloy) cast at a temperature of 1200°C (2190°F).

Considering results from the preliminary experiment (Table 2), the alloys can be ranked as follows, in the order of increasing hot-tearing susceptibility: BNF alloy, tin bronze (1A), Inco alloy, and silicon bronze (12A), the last-mentioned being considerably more susceptible than the others. Variations in pouring temperature between 1275°C (2325°F) and 1200°C (2190°F) have little if any influence on the susceptibility of 1A, 12A and Inco alloys, whereas the rating of BNF alloy increases regularly with decreasing pouring temperature. Results are highly consistent with the 1A and BNF alloys and less so with the other two.

According to the results of the main experiment presented in Tables 3 and 4, the alloys investigated can be ranked as follows so far as their hot-tearing susceptibilities are concerned:

1) High-strength yellow brass (8A) and propeller bronze are the least susceptible, as no crack at all was found in any of the bar castings;

2) leaded high-strength yellow brass (7A) has a very low susceptibility, as one of the two

melts prepared from this alloy did not show any crack, and the small defects found in some bars of the other melt may or may not have been hot-tears;

3) high-leaded tin bronze (3A) bars showed some hot-tears, but the susceptibility of this alloy is much lower than that of most alloys;

4) the 89 Cu - 11 Sn alloy has an intermediate susceptibility;

5) tin bronze (1A) and the BNF and 80 Cu - 5 Sn - 10 Pb-5 Zn alloys have a rating of 10 to 13 units higher than that of the 89 Cu - 11 Sn alloy;

6) leaded semi-red brass (5A) and leaded yellow brass (6A) are more susceptible than those of group 5, by approximately 9 units;

7) leaded red brass (4A) and Inco alloy are more susceptible than the alloys of group 6, also by approximately 9 units; and

8) silicon bronze (12A) is the most susceptible of the alloys studied, with a rating of approximately 15 units higher than the alloys of group 7.

The results of Tables 3 and 4 indicate that the pouring temperature has an appreciable influence on the hot-tearing susceptibility of many alloys. Decreasing the pouring temperature from 1200°C (2190°F) to 1100°C (2010°F) decreased the hot-tear rating by 24% in tin bronze (1A), by 16% in leaded red brass (4A), by 28% in leaded yellow brass (6A), by 29% in BNF and Inco alloys, and by 58% in the 89 Cu - 11 Sn. In all six cases an intermediate pouring temperature of 1150°C (2100°F) produced intermediate results. High-leaded tin bronze (3A) and the 80 Cu - 5 Sn - 10 Pb - 5 Zn alloy also showed a minimum crack rating in bars cast at the highest temperature, but their maximum susceptibility was found in bars cast at the intermediate temperature. A reduction in pouring temperature resulted in an increase in susceptibility of 82% for leaded semi-red brass (5A). The susceptibility of silicon bronze (12A) was not much affected by pouring temperature within the range of temperatures investigated.

There appears to be some discrepancy, in the influence of pouring temperature on the hot-tearing susceptibility, between the results from the preliminary and main experiments. However, as the two experiments were

carried out over different temperature ranges and under different experimental conditions, comparison is difficult. It must also be remembered that the pattern changes between the preliminary and final design appeared to make the final hot-tear test more severe. In order to determine whether the influence of pouring temperature is the same in both temperature ranges with the same pattern, two melts of tin bronze (1A) and two melts of BNF alloy were cast at 1275°C (2325°F), 1250°C (2280°F), 1225°C (2235°F), 1200°C (2190°F), 1150°C (2100°F) and 1100°C (2010°F), so that both ranges of temperatures were fully covered. Although this experiment is very limited, the results so obtained suggest that, in both alloys, the hot-tearing susceptibility may show a maximum in the vicinity of 1200°C (2190°F) under the present testing conditions.

With very few exceptions, the hot-tear rating increased regularly with increasing bar length. However, in all the moulds cast at 1200°C (2190°F) from the 80 Cu - 5 Sn - 10 Pb - 5 Zn alloy and from leaded semi-red brass (5A), the bars were either completely broken or not cracked at all. The moulds cast at lower temperatures exhibited the regular pattern shown by all the other alloys that were found to be susceptible to hot-tearing.

Although the final experiment was not designed to determine the maximum bar length which could be cast without cracking in the various alloys, some estimates are shown below:

| | |
|---|---|
| 18 in. and over | High-strength yellow brass (8A) propeller bronze and leaded high-strength yellow brass (7A), |
| 14 in. | High-leaded tin bronze (3A), |
| 12 in. | 89 Cu - 11 Sn alloy, |
| 10 in. | Tin bronze (1A), leaded yellow brass (6A), BNF alloy, and 80 Cu - 5 Sn - 10 Pb - 5 Zn alloy, |
| 8 in. | Leaded red brass (4A) and leaded semi-red brass (5A), |
| 6 in. | Inco alloy, |
| Less than 6 in. | Silicon bronze (12A). |

## EXAMINATION OF HOT-TEAR TEST PIECES

### Fracture Examination

The fractures of a large number of broken hot-tear bars were examined under a low-power binocular microscope and the following observations were made:

The first point of interest is that the appearance of the adjacent fractures was not the same on the ball side as on the bar side. The fractures on the ball side do not vary from alloy to alloy: they are roughly concave, and consist of a number of facets which probably correspond to the contours of the dendrites formed during solidification.

The fractures on the bar side are roughly convex and they, in general, have two characteristic aspects, both of which may be present in the same fracture. In the first case the fracture has a honeycomb appearance with roughly cylindrical cell walls terminated by a hemisphere (Figure 3). The cell walls are very thin, smooth, and oxidized. This type of fracture was mainly found in leaded red brass (4A), leaded semi-red brass (5A), leaded yellow brass (6A), and in the 80 Cu - 5 Sn - 10 Pb - 5 Zn alloy.

The other type of fracture, shown in Figure 4, consists of a number of corrugated and differently-oriented facets very much like the fractures on the ball side. However, the fractures on the bar side carry "whiskers" which stand out from the surface. This type of fracture was mainly seen in tin bronze (1A), silicon bronze (12A), and BNF and Inco alloys, although the latter frequently presents both types of fractures in the same bar and in different bars of the same mould.

### Estimation of Temperature of Fracture

In order to obtain some information about the temperature at which the fracture took place, separately-cast 1/2-in. diameter bars of leaded red brass (4A) and tin bronze (1A) were tensile-tested at each of the following temperatures: 500°C (930°F), 550°C (1020°F), 600°C (1110°F), 700°C (1290°F), and 800°C (1470°F). The specimens were heated in air over a period of 50 to 90 min to the test temperature, and soaked for 30 min before testing. The appearance of the fractures did not vary with the testing temperature and, as shown in Figures 5 and 6, is quite different from that of the hot-tear bar fractures (see Figures 3 and 4). The large facets of the fracture in Figure 6 did not contain fine "whiskers" as did the facets of the hot-tear fractures, Figure 4.

Metallographic examination of tested bars showed that the heating during the hot tensile testing was sufficient to dissolve all of the delta phase present in the cast leaded red brass (4A) and in the tin bronze (1A) tested at 800°C. This indicates that the "effective" * solidus of both alloys had been raised by heating prior to testing. Thus, the temperature of 800°C, which was thought to be a few degrees higher than the "effective" * solidus of these alloys, was somewhat lower than the solidus of the now homogenized specimens and the two sets of testing conditions are not strictly comparable. However, the tests strongly indicate that the fractures obtained on the hot-tear test coupons are true hot-tears, and not cracks occurring at temperatures below the solidus.

Metallographic Examination

A very large number of hot-tear bars, representing all the alloys investigated, were longitudinally sectioned through the hot spot. Sections of castings from early melts were taken from the bar up to a distance of approximately 6 in. from the ball. In all the alloys in which delta phase is present (because cooling was too rapid to allow homogenization of the structure), i.e., tin bronze (1A), high-leaded tin bronze (3A), leaded red brass (4A), leaded semi-red brass (5A), leaded yellow brass (6A), BNF, Inco, and the 80 Cu - 5 Sn - 10 Pb - 5 Zn (the 89 Cu - 11 Sn alloy was added later), the following phenomenon was observed. The general microstructure of the first inch of the bar measured from the ball contains appreciably less delta phase than the remainder of the bar, suggesting considerable segregation. It was realized, however, that the cooling conditions at the hot spot were conducive to a higher degree of solution of the tin in the alpha phase than is the case for the remainder of the bar, and a chemical analysis survey was, therefore,

---

* The expression "effective" solidus is used to denote the temperature at which the last copper-rich phase freezes in a casting. This may be appreciably different from the equilibrium solidus, which can be determined only upon sufficiently slow cooling to allow complete homogenization of the structure, a condition which is seldom, if ever, attained in practice. As the expression "effective" solidus refers to a copper-rich phase, it does not take into account the lead-rich phase which is found in many copper casting alloys and which remains liquid down to a temperature of approximately 320°C (610°F). However, in the context of this work, it is considered that the freezing of the copper-rich phase is the critical stage, although the presence of the liquid lead-rich phase -- sometimes in considerable quantities -- will obviously have an important effect.

carried out on two tin bronze (1A) bars. It was found that the tin contents at the hot spots were 8.3 and 8.5%, as against 9.6% for the bar average, which corresponds to a difference of 11 to 14%. The microstructure on the ball side of the metallographic specimens was coarser than that of the bar and gave no evidence of segregation.

In contrast to the previously mentioned alloys, leaded high-strength yellow brass (7A), high-strength yellow brass (8A), silicon bronze (12A) and propeller bronze castings did not show any evidence of segregation.

Lead particles, where present, are, in general, evenly distributed throughout the microstructure of the castings. However, a few specimens taken from high-leaded tin bronze (3A) bars present evidence of lead globule alignment at the hot spot of the casting, as shown in Figure 7.

Although the portion of the bar located near the hot spot had less delta phase and a lower tin content than the average, heavy segregate bands of delta phase were found at the hot spot of specimens from the majority of the tin-rich alloys. These bands of segregate were of two kinds. The first is in the form of heavy stringers of delta located at grain boundaries which are roughly perpendicular to the main axis of the bar. Examples are shown in Figures 8, 9, 10 and 11, in which the stringers of delta are accompanied or interrupted by a number of cavities. Particular care was taken to cut the metallographic specimens through external cracks so that the crack configuration and edges could be examined, and numerous samples showed cracks ending in a stringer of delta phase of the same nature as those previously mentioned. Figures 10, 12, 13, 14 and 15 are typical of this phenomenon, and again the delta stringers are roughly perpendicular to the main axis of the bar. As these delta phase stringers are seen in areas which contain, in general, little delta, and as they are essentially oriented in a direction normal to the direction of the stresses imposed on the hot spot by the contracting casting, it is suggested that the stringers are in effect completely or partially healed hot-tears.

A second type of segregate band was found at the fracture of completely ruptured castings and was exclusively on the bar side of the fracture. A few examples of this phenomenon are shown in Figures 16, 17, 18, 19 and 20. A cross-section of these fractures presents a relatively wide band of eutectoid which, in some cases, is almost continuous across the whole bar although, in general, it is a local phenomenon, the remainder of the section consisting of alpha phase with an average or less than average delta phase concentration. These eutectoid-rich bands are usually much larger than the stringers of delta mentioned previously. In numerous cases where the fracture presents a sharp peak, as in Figure 21, the microstructure of the peak itself is richer in delta phase than the underlying matrix.

In one instance, a metallographic section was prepared by lightly

grinding and polishing the face of the fracture rather than the usual transverse section. As shown in Figure 22, a considerable amount of delta phase was present, whereas all the longitudinal sections from the other 14-in. and 18-in. bars from the same melt cast at the same temperature showed no delta. This suggests that the delta distribution over the face of the fracture is more general than would appear from the longitudinal sections.

As noted, this segregation of delta on the face of the fracture appeared to be confined to the bar side of the fracture, and this probably accounts for the different appearance of this fracture as compared with the mating one on the ball side. (A similar phenomenon occurred when magnesium alloys were tested, the bar side of fracture having a black and burned appearance in contrast to the bright facets on the corresponding ball side.)

## Grain Size Determination

Several melts from the preliminary and main experiments, and covering most of the alloys studied, were examined for grain size.

It was found that the type of grains (equiaxed versus columnar) varied from bar to bar within the same mould and could not be related to the hot-tearing susceptibility. However, grains on the ball side of the fracture were more columnar and appreciably longer than those on the bar side. In cases where a columnar zone is adjacent to an equiaxed zone on the bar side, cracks tended to follow the boundary between the two zones.

In most cases, within the ranges investigated, the pouring temperature had little or no effect on the grain size, although the grain size of tin bronzes 1A and 89 Cu - 11 Sn and propeller bronze tended to decrease with decreasing pouring temperature.

In the five following: tin bronze (1A), leaded red brass (4A), 89 Cu - 11 Sn, B.N.F. and Inco alloys, the crack rating increases with increasing grain size.

## Thermal Analysis

The first step towards the understanding of the solidification mechanism (discussed later) of any alloy is the determination of the temperatures at which new phases appear during freezing. These essential data are not available for most of the alloys investigated, or, when published, are incomplete, misleading, or contradictory. For example, solidus data given in handbooks usually refer to the equilibrium solidus, which, in general, implies cooling conditions markedly different from those found in actual castings (see footnote to page 9, "effective" solidus). Thus, solidification mechanisms

based on such values may be considerably different from conditions obtained in practice.

The alloys investigated were therefore examined, using the differential thermal analysis technique, at cooling rates which varied between 1 and 100°C/min (2 and 180°F/min). The cooling rates prevailing at the hot spot of the bars used in this investigation were probably of the order of 75 to 100°C/min (135 to 180°F/min), as estimated from thermocouples located 3/8 inch from the hot spot on the ball side in order not to interfere with hot-tearing. In some cases it was found necessary to use lower cooling rates in thermal analysis to detect a number of reactions which would have been missed at the high rates (100°C/min or 180°F/min), and the values reported in Table 5 therefore correspond to a cooling rate of 10°C/min (18°F/min) which is sufficiently close to cooling rates in castings. It may be pointed out as a matter of interest that the temperatures of the beginning of the separation of alpha and delta phases are little affected by variations in cooling rates within the range considered.

The expression "thermal arrests" in this report refers to deviations in the slopes of differential curves and indicates the beginning of a transformation. In general the end of such transformations is not so well defined and could not be detected with accuracy. In Table 5, under the heading "Thermal Arrests", column A gives the temperature at which the alpha phase begins to separate, columns B and C the beginning of monotectic transformations in the Cu-Pb-Zn and Cu-Pb-Sn systems as will be seen later, and column D the beginning of the peritectic transformation in the case of tin-containing alloys. This temperature is probably only a few degrees above the temperature of the end of the transformation, which is in fact the "effective" solidus of the alloy and can be compared with solidus data given in the literature. For alloys which contain little or no tin, the values given in Column D represent the effective solidus of the alloys and were obtained upon heating, as they could not be safely assessed from the cooling curves. Column E corresponds to the beginning of the solidification of the lead-rich phase at temperatures in the vicinity of 320°C (610°F).

## DISCUSSION

### Previous Work

The factors which determine the hot-tearing behaviour of copper alloys have received little attention in the literature, and it seems appropriate to outline some of the basic principles governing this phenomenon as derived from extensive studies of ferrous and other non-ferrous alloys.

One of the most plausible theories put forward to explain the mechanism of hot-tearing is the strain theory of hot-tearing developed by Pellini (9). This was comprehensively reviewed by Dodd (10), and questioned by Saveiko (11) whose claims are far from convincing. Pellini proposes that hot-tears are formed in a hot spot when the rate of extension of the liquid films that surround the solidifying grains at temperatures slightly above or at the "effective" solidus exceeds a critical value. When a casting solidifies under conditions which hinder its free contraction, stresses are generated and transmitted along the solid portions of the casting. If parts of the casting are not completely solid, these stresses tend to produce the extension of such zones because they are the weakest. According to Pellini's theory, the rate of extension of the incompletely solid zones is the deciding factor in the occurrence of hot-tears at those points of weakness.

Among the factors which contribute to high rates of extension of the liquid films, and hence hot-tearing, Pellini mentions the following:

(1) long regions undergoing contraction,

(2) fast cooling of regions undergoing contraction,

(3) narrow hot-spot regions undergoing extension.

The influence of only the first of the above factors was systematically assessed in the present investigation, and the results fully agree with Pellini's claims. As indicated earlier, the longest bars definitely tore more readily than the short ones. The strain theory explains this phenomenon by showing that, all other factors being equal, the same number of films have to accommodate a greater extension at the critical time in the longer bars and thus the danger of tearing is increased.

Although the third factor was not systematically investigated during the development phase, bars of equal length were cast to the following diameters: 1/2, 5/8, and 3/4 in. Because the amount of metal flowing through the hot spot of the 5/8-and 3/4-in. bars is 1.5 and 2.25 times respectively that for the 1/2-in. bars, the sand in that area is heated appreciably more, and over a longer distance, than in the small bars. This causes a lengthening or "dilution" of the hot zone, and this in turn increases the number of liquid films which undergo the same absolute extension. Thus, again in agreement with Pellini's theory, the smaller-diameter bars cracked more readily. Similarly, altering the pouring temperature might have an effect on the results: a high pouring temperature might be expected to reduce the hot-tear rating by spreading the hot spot or, conversely, might increase the hot-tear rating by increasing the film life. Furthermore, in this case, there are also structural and mechanical changes taking place in the sand mould,

and the mode of solidification of the alloy and its crystal structure might be considerably modified. Thus the effect of pouring temperature is less definite and might well vary from one alloy to another, or from one casting to another, depending on which are the most critical factors for the particular case. This is supported by one of the conclusions arrived at by Bishop, Ackerlind and Pellini [12] and which reads as follows: "the effect of pouring temperature should be considered highly specific to the type of casting in question. The conclusion is based on the variety of possible effects from pouring temperature on the nature and extent of the hot spot and contraction conditions resulting from simple modification of gating and risering methods".

Besides the critical strain, another factor which must be considered is the liquid film life or the period of time during which the films undergo extension. Some alloys go through that critical period very rapidly, thus allowing little time for extension to take place before the hot spot has attained sufficient strength to withstand the contraction stresses generated within the casting. Other alloys remain in the critical stage for such a long time that an appreciable extension must be absorbed by the hot zone and danger of hot-tearing is thus greatly increased. In yet other alloys, so much liquid phase remains while the primary crystals develop sufficient strength to withstand the strain that the matrix can yield readily, and any incipient hot-tears are immediately filled by solute-rich liquid phase. Thus this class of alloys is self-healing and resists hot-tearing very well.

Amongst the factors which influence the film life are the pouring temperature as mentioned previously, the thermal conductivity of the mould and alloy, the amount and nature of the segregates which compose or are in the liquid films (a function of the alloy composition), and the liquidus-solidus range. A number of other factors may also influence the hot-tearing resistance of alloys, such as:

(a) Grain size. An increase in grain size increases the hot-tearing susceptibility [13] because large grains form a coherent network earlier in the solidification process and thus increase the effective film life. Also, with a large grain size the number of grain boundary films per unit length is appreciably reduced, thus increasing the extension that each film has to absorb and, consequently, the danger of hot-tearing.

(b) Gas content. The presence of gas in the molten alloy may decrease the hot-tearing tendency [13, 14, 15] by reducing the volumetric contraction through the formation of porosity and by forcing liquid metal into incipient tears.

(c) Thermal contraction. The thermal contraction of the solid part of the casting influences directly the extension which the liquid films in the hot spot have to absorb for a given temperature drop.

(d) Design of the casting. Whether this be a normal industrial casting or a test bar designed to induce hot-tearing, the shape of the casting, the gating, the risering, etc., also affect results by their influence on the various factors described above as they are related to each alloy, the direction and magnitude of thermal gradients, the supply of hot metal to feed incipient tears, the degree of constraint, etc.

## Comparison of Previous Work with Present Results

There are very few references in the literature to the hot-tear resistance of cast copper alloys, although there is considerable literature on the possibly related phenomenon of hot cracking during hot working. Thus Lees (13) states that "lead in β-brass is unlikely to influence hot-tearing, but in α-brass it forms films at the grain boundaries and the tendency to hot-tearing is increased". He does not mention the test used or the actual results.

More recently, Reiter (16) assessed the hot-tearing susceptibility of copper alloys in an aluminum bronze mould, by restraining the contraction, during solidification, of rods of various lengths and observing the maximum permissible restraint, i.e. length, to avoid cracking. Tin bronze (1A, 88 Cu - 10 Sn - 2 Zn), leaded red brass (4A, 85 Cu - 5 Sn - 5 Pb - 5 Zn), and phosphor bronze (90 Cu - 10 Sn) were tested with and without 0.3% sulphur and cast with 170°C (305°F) superheat. It was found that sulphur had little influence, if any, on the hot-tear resistance and all three alloys gave essentially the same results. The author concluded that this agreed with the fact that all these alloys have a wide solidification range with only a small percentage of remaining liquid at the peritectic temperature. (In fact, it would be expected that 4A would have appreciably more liquid towards the end of the peritectic reaction because of its higher lead content.) Stolarczyk (17, 18), presumably using the same type of mould, reported no significant difference in the susceptibility to tearing of tin bronze (1A, 88 Cu - 10 Sn - 2 Zn), leaded red brass (4A, 85 Cu - 5 Sn - 5 Pb - 5 Zn), and B.N.F. alloy (87.5 Cu - 7.5 Sn - 3 Pb - 2 Zn), and claimed that small additions of bismuth, iron, arsenic and antimony produced no significant variation in the hot-tearing of both tin bronze (1A) and leaded red brass (4A).

It will be noticed that the hot-tear results reported by Reiter and Stolarczyk are not in complete agreement with the results of the present investigation which shows that, although the susceptibilities of tin bronze (1A) and B.N.F. alloy are the same, that of leaded red brass (4A) is appreciably higher. However, testing in a metal mould may be so drastic that the sensitivity of the test is greatly reduced and discrimination between alloys is thus more difficult. This is supported by Lees [13], who studied the hot-tearing tendencies of aluminum casting alloys in sand moulds and copper dies: "the test in sand moulds discriminates clearly between aluminum alloys which are particularly prone to tearing and probably gives sufficient discrimination between all the aluminum alloys to indicate their susceptibility to the defect when sand-cast. The die-cast test piece does not discriminate between aluminum alloys less prone to the defect". Furthermore, the rigidity of the metallic mould may be such that cracks may form after the casting has solidified, and it is not always easy to establish if a crack formed before or after solidification is completed. This danger also exists in sand moulds but not to the same extent, as shown by one experiment carried out with $CO_2$ moulds on tin bronze (1A) cast at 1150°C (2100°F). The average crack rating per pair of moulds is 12-1/2 (Table 3) in sand moulds, whereas it was 28 for $CO_2$ moulds. If Pellini's [9] statement that "the loads developed at the time of hot-tearing are of relatively low order (30-200 psi) if complete tearing of the test section is obtained" holds for copper alloys, it seems that the green sand moulds used in this investigation were sufficiently strong to produce complete hot-tearing of the bars, as the restraint imposed on the bars was calculated to be at least of the order of 300 psi. Thus, tearing in excess of that produced by the green sand moulds probably took place at a temperature lower than the solidus.

Novikov et al. [19] studied the influence of basic alloying elements and certain impurities on the hot shortness of one brass and three bronzes, by means of ring specimens previously used for aluminum alloys. It is difficult to be sure of the basic compositions used, but it seems that they are: 80 Cu - 17 Zn - 3 Si for the brass, and 85 Cu - 3 Sn - 4 Pb - 7 Zn - 1 Ni, 85 Cu - 5 Sn - 4 Pb - 5 Zn - 1 Ni, and 80 Cu - 3 Sn - 4 Pb - 12 Zn - 1 Ni for the bronzes. Similarly, although the test conditions are not clearly defined, it appears that the authors used a mould of the Singer-Jennings type [10].

It was found that increasing the zinc content of brass from 15.5 to 17.5% decreased the hot shortness to a certain extent, and that an increase in silicon content from 2.5 to 4% drastically reduced the hot-tearing susceptibility. Hot shortness is not significantly influenced by increasing the Al content from 0.01 to 0.1% or by adding 1 to 3% Pb. In the 85 Cu - 3 Sn - 4 Pb - 7 Zn - 1 Ni bronze, a tin content of 4.5% reduced the susceptibility appreciably when compared to alloys with 2.5 to 4% Sn, and an increase in zinc from 6.5 to 9% decreased the hot shortness slightly; an increase in aluminum from 0.01 and 0.1% increased markedly the hot-tearing tendency of this alloy. In the case of leaded red brass, increasing the tin and zinc

contents resulted in a reduced susceptibility. However, increasing the tin content of the 80 Cu - 3 Sn - 4 Pb - 12 Zn - 1 Ni bronze increased the susceptibility sharply, whereas increasing the zinc resulted in some improvement. As only one of the alloys studied by Novikov is comparable to those investigated in the present study, and the compositions are not clearly defined, it is not possible to give an effective comparison of results.

Temperature of Hot-Tearing

Since, by definition, the term hot-tearing is used to describe supra-solidus cracking (before solidification is completed) [1], it is desirable that the temperature at which cracking takes place in copper alloys be determined. However, in view of the danger of obtaining false temperature readings [9], on the one hand, and of the difficulty of determining when cracks are formed, on the other, it was decided to try to obtain the same information by means of fracture and metallographic examinations. It must be mentioned at this point that the oxidation of the fracture surface does not prove that the fracture took place above the solidus, because oxidation of a copper alloy surface can take place in air several hundred degrees below the solidus (this was confirmed by a short hot-stage microscope experiment). As mentioned earlier, the fractures of some alloys have a honeycomb appearance whereas others show very fine whiskers of metal standing out from the facets, and metallographic examination showed both these to be tin-rich material. Tensile tests carried out at temperatures up to 800°C (1470°F) on test bars of tin-bronze (1A) and red brass (4A) produced fractures which are entirely different from those examined after the hot-tear tests. Whatever the reason may be for the difference in the fractures of the hot-tear bars, and whether or not the honeycomb appearance of some fractures was caused by gas evolution or by other factors, it is clear that both fracture configurations indicate that the fractures were at least initiated when there was still some tin-rich liquid left in the microstructure. In addition, the metallographic examination of hot-tear specimens showed heavy segregation of delta phase (in tin-containing alloys) to the areas where fractures were about to take place, and this could only occur at temperatures where the tin-enriched material was still relatively free to migrate. This temperature must be above the "effective" solidus of the alloy. It is important to note here that the "effective" solidus is more important than the equilibrium solidus because it represents what occurs in the casting at the time of solidification whereas the equilibrium solidus temperature has very little relation to the casting conditions.

External vs Internal Hot-Tears

The hot-tears studied in this investigation are those which are commonly referred to as external hot-tears because they reach the surface of the castings. Tears of this type are caused by external restraint produced by cores, sand, inserts, or anything which restricts the casting contraction after some part of it has solidified. However, in larger castings, internal hot-

tears [2, 20] may occur which differ from the external ones only by their locations in the casting [10]. The internal tears, as the name implies, are not open to the surface of the casting and are not, therefore, detected by visual examination. As mentioned by Cibula [20], a special type of internal hot-tearing results in layer porosity due to the continuation of both solidification and cooling contractions after mass feeding has become impeded, and this view is supported by Ruddle [21]: "it is not difficult to imagine that during this critical stage, when coherence between the crystals is being established, movement of a mass of metal might occur in one region of the casting, but that movement of an adjacent mass in conformity might be prevented because coherence is more firmly established in this second region; as the result, the first mass moves away from the second and a cavity forms between them. The plate-like fissure thus created is really a kind of internal hot tear. Because the casting is as yet not fully solid, a certain amount of liquid metal usually seeps into the cavity, which therefore normally takes the form of a layer of discrete or inter-connecting holes in the fully solid casting". Cibula states that, because open external hot-tears are exposed to atmospheric pressure, they would be healed with more difficulty than internal tears, whereas Beckius [2] holds that internal tears form very late during solidification when healing is no longer possible. However, the latter author is dealing with steel castings which have a much shorter freezing range. The metallographic examination carried out during this investigation revealed numerous internal tears within the ball of the test bar, and those, with very few exceptions, did not show any concentration of delta phase or a tendency to be healed, whereas the external tears did. Presumably the ability of an internal tear to heal is largely a function of the availability of liquid metal from another part of the casting.

Discrepancy between Main and Preliminary Experiments

Results from the preliminary (Table 2) and main (Table 3) experiments are not directly comparable, for a number of reasons: a) the 6-inch bar used in the preliminary experiment was replaced by a 12-inch bar in the main experiment, and this increased the rating appreciably; b) the standards with which the specimens were compared were changed between the two experiments, to give a better range for assessment; c) the casting temperature was an average of 85°C (150°F) higher in the first experiment than in the second; and d) the pattern design was altered before starting the main experiment.

Discrepancy from Melt to Melt

The results of Table 3 show a generally increasing trend in crack rating as the melt numbers increase (i.e. as the investigation progressed), for tin bronze (1A), leaded red brass (4A), and the Inco and 80 Cu - 5 Sn - 10 Pb - 5 Zn alloys. Because melts were generally prepared from remelted casting sections from a previous melt, the most obvious explanation of this

phenomenon is that the metal became gradually contaminated with an element or elements which increase its hot-tearing tendency. However, a specimen from every melt of leaded red brass and Inco alloy was spectrographically analysed for elements other than those reported in Table 1. Results of this analysis failed to show any systematic variation from melt to melt. In order to check the possibility of contamination, melt No. 1039 was prepared exclusively from new metal; its crack rating was the second highest for that alloy, thus indicating that the effect is unlikely to be due to contamination. Another possible explanation is that the observers, being more trained in the later stages of the work, may have become more critical as the experiment progressed, thus giving higher ratings. Although this is not impossible it is unlikely, as they continuously referred to the pre-established crack standards during the rating operations. Furthermore, even in the late stages of the investigation some melts were found with a lower rating than previous melts.

The chemical composition results of Table 1 were analysed in order to determine if variations in analysis could have caused those differences in crack rating. Because of the complexity of the alloys this was unsuccessful. A brief analysis of the sand properties: hardness, permeability, moisture content, and green strength, failed to show a definite relationship with crack rating. Thus, no completely satisfactory explanation of this variation in rating between various melts can be offered. Amongst the factors which were not controlled during this experiment, the gas content of the melt could have had a pronounced influence on the hot-tearing tendency. Melts were flushed with nitrogen for a fixed period at a fixed rate and the amount of nitrogen passed through the melts was several times that used in commercial foundries, but no test of the efficiency of the degassing operation was carried out. Separately-cast test bars (Dow pattern) and hot-tear bars were cast from several melts before and after degassing and no definite trend could be detected, either in the mechanical properties or in hot-tearing susceptibility. In spite of those restrictions, the efficiency of the degassing treatment may have been higher in the last melts than in the first ones and this may have increased the hot-tearing tendency, as mentioned by Lees (14, 15) in the case of certain aluminum alloys. It was found that grain diameter varies appreciably from melt to melt and, as mentioned earlier, grain size and crack rating vary in the same direction. However, it is not known if such a grain size variation is sufficient to account for the difference in crack rating results.

## Assessment of Crack Rating Method

It is fully appreciated that the method used in this investigation for rating the hot-tearing susceptibility of sand-cast copper alloys is somewhat arbitrary. Furthermore, as suggested by studies carried out by different investigators on ferrous and other non-ferrous alloys, it is possible that another rating method would have yielded different results. However, as the bars were cast in a common sand mixture and as the results showed reasonable reproducibility in spite of the limitations described in previous sections,

it is felt that the test can definitely discriminate between alloys which are shown in Tables 3 and 4 to be significantly different. For instance, it is considered that the test may not differentiate between tin bronze (1A) with a crack rating of $37\frac{1}{2}$ and B.N.F. alloy which has a rating of $40\frac{1}{2}$, but it readily discriminates between tin bronze (1A) - $37\frac{1}{2}$ - and leaded red brass (4A) with a crack rating of 57. In other words, if, because of design, hot-tearing is anticipated in a sand casting, the foundryman who has a choice of alloys should select the alloy which the present investigation has shown to be appreciably less susceptible to hot-tearing than the others. The test also shows that the pouring temperature may significantly influence the hot-tearing susceptibility of certain copper alloys, so that this is another variable worthy of attention when hot-tearing problems are encountered in the foundry.

Influence of Constitution on Hot-Tearing

As mentioned, perhaps the most important factors in hot-tearing are the amount of liquid and the time during which liquid films are present as the casting solidifies. It is therefore worthwhile to examine the constitution diagrams of the alloys to see what information can be obtained on the above. Unfortunately, in the case of the industrial cast copper alloys, many of these are from systems having at least three components and the data on such systems are practically non-existent. Also, particularly in the case of tin-rich alloys, the cast structures show a considerable departure from the equilibrium structures represented by the constitution diagram. As mentioned earlier, the concept of "effective" solidus has been used in an attempt to simplify the understanding of hot-tearing in lead-containing alloys.

In spite of all these difficulties, an attempt is made to explain some of the possible reactions taking place as the alloys solidify. This is based on differential thermal analysis, as explained earlier.

(a) Mode of Solidification of the Various Alloys

The significance of the various arrest temperatures will now be discussed in terms of the binary equilibrium diagrams (Figures 23 to 26), the ternary Cu - Sn - Pb (Figures 27 and 28) and Cu - Zn - Pb (Figure 29) diagrams, and the data shown in Table 5. A word of caution is required when the diagrams of Figures 27 and 29 are considered, because some points on those diagrams are known with certainty, whereas others are not and were placed in convenient and probable locations. The known points - capital letters - are those obtained from binary equilibrium diagrams; the remainder - small letters - are based on experiment, inference and extrapolation and are therefore subject to some error.

Alloy 1A is considered as a binary 90 Cu - 10 Sn alloy. For the composition given in Table 5, freezing starts by the separation of copper-rich crystals at 986°C (1306°F) and this continues until 782°C (1440°F) which

corresponds to the peritectic formation of β at 798°C (1468°F) in the binary Cu - Sn system (Figure 23). Thus the remaining tin-rich liquid in 1A reacts with α to give β. This occurs at a constant temperature in the binary system, but in the ternary Cu - Sn - Zn system the point is not invariant, so that the reaction occurs probably over a short range of temperature until the liquid is used up, and the alloy is then completely solid. Subsequently, this peritectic β transforms eutectoidally to γ and this to δ but these are all solid state transformations and hence, by definition, play no part in hot-tearing. Thus, in this alloy, the β formation corresponds to the solidus. It should be remembered that the amount of liquid present during this last stage of solidification is indicated by the amount of δ which is observed in the microstructure and this is somewhat less than the volume of β (and therefore the tin-rich liquid) from which it was formed through the $\beta \rightleftharpoons \alpha + \gamma$ and $\gamma \rightleftharpoons \alpha + \delta$ eutectoid reactions. For the sake of uniformity and comparison with other alloys, this is plotted on the ternary Cu - Sn - Pb diagram of the liquidus surfaces in Figure 27, where it will be seen that after the first separation of α, which occurs at 986°C (1806°F) at the symbol denoting 1A, the composition of the liquid moves down the line AK until it reaches the point K which represents the start of the β peritectic transformation (occurring in this case at 782°C (1440°F) rather than at 798°C (1468°F), because of the effect of zinc). A similar mode of freezing also occurs in the case of the 89 Cu - 11 Sn alloy.

In the case of alloy 3A the reactions are more complex. As shown by Table 5 and Figure 27, the first separation of copper-rich crystals occurs at 950°C (1742°F) at the point on the Ani liquidus surface represented by the symbol denoting 3A. Cooling causes further separation of alpha, and the composition of the liquid moves towards the line ni. The line ni forms part of a curve CnimjD which represents a miscibility gap of lead-rich phases which can best be understood by referring to the binary Cu - Pb diagram (Figure 24). (Additions of lead to copper reduce the liquidus temperature continuously along AC (Figure 27) to C, the miscibility limit at 36% Pb and 953°C (1748°F); see also Figure 24. At this point, a second liquid appears at D which contains 92.5% Pb and results from the monotectic transformation along CD.) When the composition reaches ni at 866°C (1590°F) for the composition given in Table 5, according to Figure 28 (a more detailed section) the composition of the liquid phase is about 17% Pb and 12% Sn. If, as seems reasonable, none or very little of the original 10% Pb has been deposited with the α phase, this lead enrichment of the liquid from 10 to 17% corresponds to a reduction in the liquid volume to 60% of the original, which means that, at this point, only 40% of the alloy is solid. Once ni is reached a second liquid phase is formed across the miscibility gap as a lead-rich liquid of composition between D and j (Figure 27), and this is accompanied by the separation of a considerable amount of alpha. Further cooling causes the composition of the tin-rich liquid to move along ni towards i, and that of the lead-rich liquid along Dj towards j, resulting in the precipitation of more α. When the tin-rich liquid reaches the point i at 767°C (1412°F), the lead-rich liquid has

reached j at the same temperature. At the point i, peritectic β is formed by the reaction of α with the tin-rich liquid, and, for this alloy, this point is invariant according to the phase rule (f = n - p + 1) since there are three components, Cu, Sn and Pb, and four phases, α, β, tin-rich liquid and lead-rich liquid. This alloy therefore substantially completes its solidification at this point, although there must be at least 10% lead-rich material still in the liquid form. Further cooling causes changes in this liquid, which is essentially similar to the lead-rich liquid of the Cu - Pb system, giving some further formation of small amounts of copper-rich α and the eventual freezing of the lead-rich Cu - Pb eutectic at about 326°C (618°F). Theoretically, the composition of the lead-rich phase should move along jl and then proceed along the eutectic valley joining $E_2$ (the Cu - Pb eutectic) and the ternary Sn - Pb - Cu eutectic, until the last remaining liquid freezes at point e, at about 180°C (356°F). In fact, this reaction does not go to completion, and other workers [6] have given the freezing point of the lead-rich phase at 314°C (597°F).

The same basic explanation also holds for the solidification of alloys 4A, 4A + 5% Pb, 5A, B.N.F., and Inco, with the following reservations caused by the fact that all these alloys contain zinc:

(a) This additional component gives the system another degree of freedom so that points such as i, corresponding to the monotectic four-phase reaction, are no longer invariant, and these transformations occur over a range of temperature.

(b) As the zinc content increases, the effect of zinc on the constitution becomes more important. Indeed, in all alloys containing more than 4% zinc, another thermal arrest point was found in the region of 890°C (1635°F) which possibly corresponds to the formation of a first lead-rich liquid in the miscibility gap of the Cu - Pb - Zn system (Figure 29), which occurs at a slightly higher temperature than in the Cu - Pb - Sn system.

(c) A similar additional arrest occurred at 812°C (1493°F) in the case of the Inco alloy, which may have been due to some change in the separation of the lead-rich phase caused by the 2% nickel in this alloy.

(d) In the case of alloy 5A, no arrest corresponding to the peritectic formation of β was detected, but a small amount of δ was observed in the microstructure, presumably coming from this source.

Thus, in all the above alloys, the amount of tin-rich liquid phase taking part in the formation of β, which is taken as the "effective" solidus, is primarily dependent on the tin content, and is represented in the room-temperature structure by δ. Similarly, the amount of lead-rich phase which is present both during and for a long time after the solidification of the last copper-rich phase is primarily dependent on the lead content, and is represented in the room-temperature structure by lead globules.

With regard to alloy 6A, the solidification of the high zinc (22%) alloys in the ternary Cu - Zn - Pb diagrams (Figure 29) is not dissimilar to the mechanism described previously. Peritectic β is formed at K' at 903°C (1657°F) in the Cu - Zn system, and the miscibility gap of the Cu - Pb system extends into the diagram in the same way as in the Cu - Sn - Pb system just discussed. Thus, crystallization of α first starts at 948°C (1740°F) for this alloy, as shown in Table 5, and a lead-rich liquid phase separates from the melt at 893°C (1640°F). A small amount of a third constituent, thought to be a form of tin-rich δ, can be seen in the microstructure. In any case the amount is small, and a very faint arrest point was detected at 775°C (1427°F) in the thermal analysis. Thus, in this case, the final amount of liquid at the "effective" solidus may be influenced by either the tin or the zinc content, and is indicated by the amount of this modified δ phase in the microstructure. As before, the amount of lead-rich phase present during and after the solidification of the last copper-rich phase is primarily dependent on the lead content, and is shown by the number of lead globules in the microstructure.

In the case of alloys other than the tin bronzes, the following conditions apply. In general, all these alloys show relatively good hot-tear resistance, and have a relatively short freezing range. Thus, the changes taking place during the solidification of these alloys have not been so critically examined. The silicon bronze is the exception to this group, since it had the worst crack rating of all the alloys.

As the chemical compositions of alloys 7A and 8A are close, both alloys are assumed to solidify by the same mechanism, which is probably as follows: These alloys are essentially similar to binary copper-zinc alloys with over 40% zinc, in accordance with Guillet's [27] "coefficient of equivalence", and freeze as a β solid solution (Figure 25). The results of Table 5 support this assumption, as only one break was noticed in the cooling curves at 890°C (1634°F) - compared to 880°C (1616°F) as given in the literature [7] - which is below the temperature of the β peritectic transformation, i.e. 903°C(1657°F). The solidus values obtained upon heating are essentially similar to those given in the literature [7], 860°C (1580°F) against 862°C (1583°F). Thus these alloys solidify over a temperature range of 30°C (54°F) by simple separation of β. Transformations taking place in the solid state are of no interest in this particular case.

In the thermal analysis of silicon bronze (12A), only two arrests were detected, at 1010°C (1850°F) and 907°C (1665°F). The first point would correspond to the beginning of the separation of the copper-rich $\alpha$ phase, and the second probably to the beginning of the formation of a silicon-rich phase (Figure 30), giving a total solidification range of about 100°C (180°F).

The solidification mechanism of propeller bronze is probably simply related to the binary Cu - Al diagram (Figure 31), solidification starting by the formation of $\alpha$ or $\beta$ solid solution, depending on the composition, and ending, in both cases, at the eutectic separation of $\alpha$ and $\beta$ at a temperature of about 1035°C (1895°F).

(b) Influence of Mode of Solidification on Hot-Tearing

Although it is highly speculative, an attempt will now be made to establish a relationship between the above discussion and the hot-tear results, particularly for the tin bronzes. This is done, not so much to explain the observed phenomena, but in the hope that it might be used to influence the future "design" of copper casting alloys. These arguments are based on the solidification range (i.e., temperature between precipitation of first $\alpha$ and the end of the $\beta$ peritectic reaction or effective solidus); the amount and type of the liquid phase present during the final stages of solidification; and the speculation that increasing the zinc has some effect on the solid phase present at high temperatures, which reduces its hot-tear resistance.

The bronzes will be considered in comparison with the hot-tear rating of 1A, because this alloy formed the basis for the solidification discussions.

Alloy 1A: 88 Cu - 10 Sn - 2 Zn

Hot-Tear Rating, 38; Solidification Range, 204°C (367°F)

This alloy has no liquid phase at temperatures below that of the end of the $\beta$ peritectic reaction.

Alloy 89 Cu - 11 Sn

Tear Rating, 27; Solidification Range, 205°C (370°F) approx. (from equilibrium diagram and thermal analysis data)

This alloy was made up, keeping the copper content the same as in 1A, and replacing the zinc by tin. It will be seen that the tear rating is substantially better than that of 1A, and it is proposed that this is due to the elimination of zinc from the alloy, since the solidus and the mode of solidification are about the same for the two alloys.

Alloy 3A: 80 Cu - 10 Sn - 10 Pb

Tear Rating, 8; Bulk Solidification Range, 183°C (330°F)

The addition of 10% Pb has resulted in a substantial improvement to the tear rating of the previous alloy. This is attributed to a slight reduction in the solidification range, and a complete change in the mode of freezing caused by the presence of 10% Pb. Because of the large quantity of tin-rich and lead-rich liquids (at either side of the miscibility gap), it is suggested that the bulk material remains "plastic" over the hot-tear range and the feeding of incipient hot-tears is readily achieved. The work of Ekbom (29) and Malmberg (30) also suggests that there may be relatively little contraction during the separation of $\alpha$ derived from the monotectic reaction, and this would, of course, reduce the strain at the hot spot and hence improve the hot-tear rating.

Alloy 4A + 5% Pb: 80 Cu - 5 Sn - 10 Pb - 5 Zn

Tear Rating, 40; Bulk Solidification Range, 217°C (390°F)

Compared to 3A, it will be seen that the addition of 4.5 Zn at the expense of the tin content has caused a marked deterioration in the hot-tear resistance. It is proposed that this is due to the increase in the solidification range, to a reduction in the amount of tin-rich liquid during the last stages of solidification which might heal incipient shrinkage, and to some deleterious effect of zinc on the hot-tear resistance. It is suggested that, in the presence of zinc, the solidifying $\alpha$ dendrites are less readily deformed at temperatures above the effective solidus, and may also be more subject to brittle failure under the contraction stresses. Similarly, the matrix may be able to transmit strain earlier and, by transmitting a greater proportion of the total contraction of the freezing section to the hot spot, may cause proportionately greater extension and strain at the hot spot, giving greater hot-tear damage.

It should also be mentioned that, in the alloys containing more than 2.5% Zn, there were indications of another thermal arrest, suggesting changes in the separation of the lead-rich phase in the region of the miscibility gap. However, this is not believed to have much effect on hot-tearing, since similar alloys with 2% Zn (B.N.F.), which did not show this arrest, gave similar hot-tear ratings.

Alloy 4A: 85 Cu - 5 Sn - 5 Pb - 5 Zn

Tear Rating, 57; Bulk Solidification Range, 250°C (450°F)

Compared to 4A + 5% Pb, reduction of the lead content by 5% has caused an increase in the hot-tear rating of 17 points. This is attributed to the increase in the bulk solidification range, to some reduction in "plasticity" and the ability to heal incipient cracks, and possibly to some increase in the bulk contraction caused by the reduction in lead content.

B.N.F. Alloy: 87.5 Cu - 7.5 Sn - 3 Pb - 2 Zn
Tear Rating, 40; Bulk Solidification Range, 239°C (430°F)

It is proposed that the improved tear rating compared to 4A is due to the lower bulk solidification range, the increase in tin, and the reduction in zinc content. The reduction in lead content would be expected to lower the tear resistance, but presumably this effect was more than counteracted by the other three.

Inco Alloy: 84.5 Cu - 6.5 Sn - 3.5 Pb - 3.5 Zn - 2 Ni
Tear Rating, 58; Bulk Solidification Range, 257°C (462°F)

This alloy is similar to B.N.F., and the worse hot-tear characteristics might be attributed to the increased bulk solidification range, and possibly to the slightly higher zinc content and lower tin content counteracting the slight beneficial effect to be expected from the additional 1% Pb. However, as discussed earlier, an additional arrest was noted in the region of the miscibility gap, which suggests that nickel is modifying the solidification characteristics. It is proposed, therefore, that the 2% nickel may be largely responsible for the somewhat poor results obtained with this material.

Alloy 5A: 81 Cu - 3 Sn - 7 Pb - 9 Zn
Tear Rating, 49; Bulk Solidification Range, 227°C (410°F)

This alloy is between 4A and 4A + 5% Pb in lead content, and indeed does have an intermediate hot-tear rating. It is suggested that increasing zinc beyond, say, 5% has a less deleterious effect than increasing zinc at lower levels, and that the reduction of tin to 3% has had only a minor deleterious effect.

Alloy 6A: 72 Cu - 1 Sn - 3 Pb - 24 Zn
Tear Rating, 46; Bulk Solidification Range, 173°C (312°F)

Because of the high zinc content, which puts this material in the class of alpha brass, rather than bronze (gunmetal), it is unlikely that the various elements will have the same effect in the two systems. It is proposed that, in this alloy, the relatively poor hot-tear resistance is related to the high temperature properties of the zinc-containing $\alpha$ phase, and to the presence of relatively small but critical amounts of liquid during the last stages of solidification. Also, the effective solidification range is much longer - 173°C (312°F) - than in the binary Cu - Zn system.

Alloy 7A: 61 Cu - 0.75 Sn - 0.75 Pb - 35.5 Zn - 1 Fe - 0.75 Al - 0.25 Mn
Tear Rating, 3; Bulk Solidification Range, 30°C (54°F)

This alloy is similar to Alloy 8A, and the two are therefore discussed together.

Alloy 8A: 58 Cu - 39.25 Zn - 1.25 Fe - 1.25 Al - 0.25 Mn
Tear Rating, 0; Bulk Solidification Range, about 30°C (54°F)

Both alloys are essentially β brasses at the freezing point and have excellent hot-tear resistance. This is attributed to the short solidification range, and to the good high-temperature ductility of the β phase. In comparing alloys 6A and 7A, it is interesting to note that, in order to avoid hot shortness during hot working operations, it is usual to limit the lead content to 0.02% in α brasses, but that β brasses containing to 2.0% Pb and 1% Sn are readily hot worked into forgings, etc. While it is appreciated that hot-tearing and hot cracking are not the same phenomenon, it is considered that they may be related. It is suggested that this gives some support to the earlier proposals that small additions of zinc deleteriously affect the hot-tear rating by modifying the properties of the original α dendrites, and that the ductility or "plasticity" of the matrix during solidification influences the hot-tearing characteristics.

Propeller Bronze: 82 Cu - 4 Fe - 9 Al - 4 Ni - 1 Mn
Tear Rating, 0; Solidification Range, 23°C (41°F)

The excellent hot-tear resistance is attributed to the short solidification range.

Alloy 12A: 87 Cu - 1 Sn - 4 Zn - 2 Fe - 1 Al - 1 Mn - 4 Si
Tear Rating, 73; Solidification Range, 103°C (185°F)

Again, this represents a different class of material, and, while the reason for the very poor tear resistance is not known, it is presumably associated with the high silicon content, which appears as a second phase in the microstructure. The solidification range of this alloy is 103°C (185°F) and this is relatively short compared to the tin bronzes. However, in some systems, maximum hot-tear rating is often found at compositions corresponding to intermediate solidification ranges.

## CONCLUSIONS

A test and a rating method have been developed to assess the hot-tearing susceptibility of various copper alloys.

Thirteen industrial and experimental copper alloys were examined, and a wide range of hot-tearing susceptibility was found as tabulated below:

| Alloy | Nominal Composition | Hot Tear Rating |
|---|---|---|
| Propeller Bronze | 82 Cu - 4 Fe - 9 Al - 4 Ni - 1 Mn | 0*) )(Best) |
| 8A | 58 Cu - 39.25 Zn - 1.25 Fe - 1.25 Al - 0.25 Mn | ) 0*) |
| 7A | 61 Cu - 0.75 Sn - 0.75 Pb - 35.5 Zn - 1 Fe - 0.75 Al -0.25 Mn | 3 |
| 3A | 80 Cu - 10 Sn - 10 Pb | 8 |
| 89-11 | 89 Cu - 11 Sn | 27 |
| 1A | 88 Cu - 10 Sn - 2 Zn | 38 |
| 4A+Pb | 80 Cu - 5 Sn - 10 Pb - 5 Zn | 40** |
| B.N.F. | 87.5 Cu - 7.5 Sn - 3 Pb - 2 Zn | 40** |
| 6A | 72 Cu - 1 Sn - 3 Pb - 24 Zn | 46 |
| 5A | 81 Cu - 3 Sn - 7 Pb - 9 Zn | 49 |
| 4A | 85 Cu - 5 Sn - 5 Pb - 5 Zn | 57 |
| Inco | 84.5 Cu - 6.5 Sn - 3.5 Pb - 3.5 Zn - 2 Ni | 58 |
| 12A | 87 Cu - 1 Sn - 4 Zn - 2 Fe - 1 Al - 1 Mn - 4 Si | 74***(Worst) |

* Corresponds to no hot-tearing in bars 18 in. long or less.
** Corresponds to some hot-tearing in bars less than 10 in. long.
*** Corresponds to some hot-tearing in bars only 6 in. long.

While the limitations of individual hot-tear tests are well known, it is considered that the above rating should serve as a general guide to enable foundrymen to select alloys with the best hot-tear resistance where this may be important in a particular casting design.

In general, it is considered that the strain theory of hot-tearing as developed by Pellini et al. offers the best rationalization of the phenomenon, and the mechanism of hot-tearing in copper alloys is discussed in general terms. The influence of composition as it affects the mode of solidification is related to the hot-tear results obtained, although this treatment is limited by the lack of available information in certain fields.

From this type of study, it may be possible to design alloys of improved hot-tear resistance, or to anticipate hot-tearing difficulties in new alloys designed from other considerations.

## REFERENCES


1. R.A. Dodd, W.A. Pollard and J.W. Meier, "Hot-Tearing of Magnesium Casting Alloys", Transactions AFS 65, 100-117 (1957).

2. K. Beckius, M.C. Flemings and H.F. Taylor, "A Study of Hot-Tearing in Steel Castings", J. Steel Casting Research, No. 19 (Oct. 1960).

3. H.F. Hall, "The Strength and Ductility of Cast Steel During Cooling from the Liquid State in Sand Moulds", 3rd Special Report No. 23, Steel Castings Research Committee, The Iron and Steel Institute, pp. 73-85 (1938).

4. C.W. Briggs, "Hot-Tear Formation", chapter in "Metallurgy of Steel Castings" (McGraw-Hill Book Co., Inc., New York, 1946), pp. 317-338.

5. F.A. Brandt, H.F. Bishop and W.S. Pellini, "Solidification of Various Metals in Sand and Chill Moulds", AFS Trans. 62. 646-653 (1954)

6. J.G. Kura and R.M. Lang, "Mechanical and Physical Properties of Three Low-Shrinkage, Copper-Base Casting Alloys", ASTM Proceedings 58, 775-790 (1958).

7. W.H. Johnson and J.G. Kura, "Mechanical and Physical Properties of Five Copper-Base Alloys", ASTM Proceedings 60. 796-811 (1960).

8. ASM Metals Handbook, 1, "Properties and Selection of Metals" (1961).

9. W.S. Pellini, "Strain Theory of Hot-Tearing", The Foundry 80, 125-133, 192, 194, 196, 199 (Nov. 1952).

10. R.A. Dodd, "Hot-Tearing of Castings: A Review of the Literature", Foundry Trade J. 101, 321-331 (1956).

11. V.N. Saveiko, "Theory of Hot-Tearing", Russian Castings Production, 453-456 (Oct. 1961).

12. H.F. Bishop, C.G. Ackerlind and W.S. Pellini, "Metallurgy and Mechanics of Hot Tearing", A.F.S. Trans. 60, 818-833 (1952).

13. D.C.G. Lees, "The Hot-Tearing Tendencies of Aluminum Casting Alloys", J. Inst. Metals 72, 343-364 (1946).

14. D.C.G. Lees, "Note on the Effect of Dissolved Gas on the Hot-Tearing of Aluminum Casting Alloys", J. Inst. Metals 73, 537-540 (1947).

15. D.C.G. Lees, "Factors Controlling the Hot-Tearing of Aluminum Casting Alloys", Foundry Trade J. 87, 211-220 (August 18, 1949).

16. H. Reiter, "The Influence of Sulphur on the Castability, Tensile Properties and Pressure-Tightness of Sand-Cast Bronzes and Gunmetals", The Brit. Foundryman 51, 2-10 (1958).

17. J.E. Stolarczyk, "The Structure and Properties of Sand-Cast Gunmetals", The Brit. Foundryman 53, 531-548 (1960).

18. J.E. Stolarczyk, D.A. Hudson and D. Ashbolt, "The Influence of Bismuth, Iron, Arsenic and Antimony in Sand-Cast Gunmetals", The Brit. Foundryman 53, 482-499 (1960).

19. I.I. Novikov, L.B. Kogan and A.E. Misyutin, "Hot Shortness in Copper Alloys for Cast Fittings", Russian Castings Production, 473-474 (Oct. 1962).

20. A. Cibula, "Influence of Grain Size on Structure, Pressure-Tightness and Tensile Properties of Sand-Cast Bronzes and Gunmetals", Foundry Trade J. 98, 713-726 (1955).

21. R.W. Ruddle, "The Solidification of Castings", Monograph and Report Series No. 7, the Institute of Metals, New York (1957), p. 293.

22. M. Hansen, "Constitution of Binary Alloys", McGraw-Hill Book Company, Inc., New York (1958).

23. ASM Metals Handbook, 1200 (1948).

24. V.S. Breisemeister, "Miscibility Gap in the Lead-Copper and Lead-Copper-Tin Systems", Z. für Metallkunde 23, 225-230 (1931).

25. D. Hanson and W.T. Pell-Walpole, "Chill-Cast Tin Bronzes", Edward Arnold and Co., London (1951).

26. H. Niclassen, "Forschungsarbeiten zur Metallkunde", Heft 7, Gebr. Borntraeger, Berlin (1922).

27. L. Guillet, Rev. de Métallurgie, 1 (1905); 2, 243 (1906); 17, 561-567 (1920). Also Chem. Met. Eng. 24, 177, 609 (1921).

28. A.G.H. Andersen and A.W. Kingsbury, "Phase Diagram of the Copper-Iron-Silicon System from 90 to 100 Per Cent Copper", AIME Transactions 152, 38-47 (1943).

29. L. Ekbom, "Influence of Increased Lead Content on Pressure-Tightness of Leaded Gunmetal", Foundry Trade J. 109, 355-361 (1960).

30. T. Malmberg, "Determination of the Specific Volume of Liquid Copper-Lead Alloys", J. Inst. Metals 89, 137-139 (1960-61).

===

AC:JOE:(PES) lc

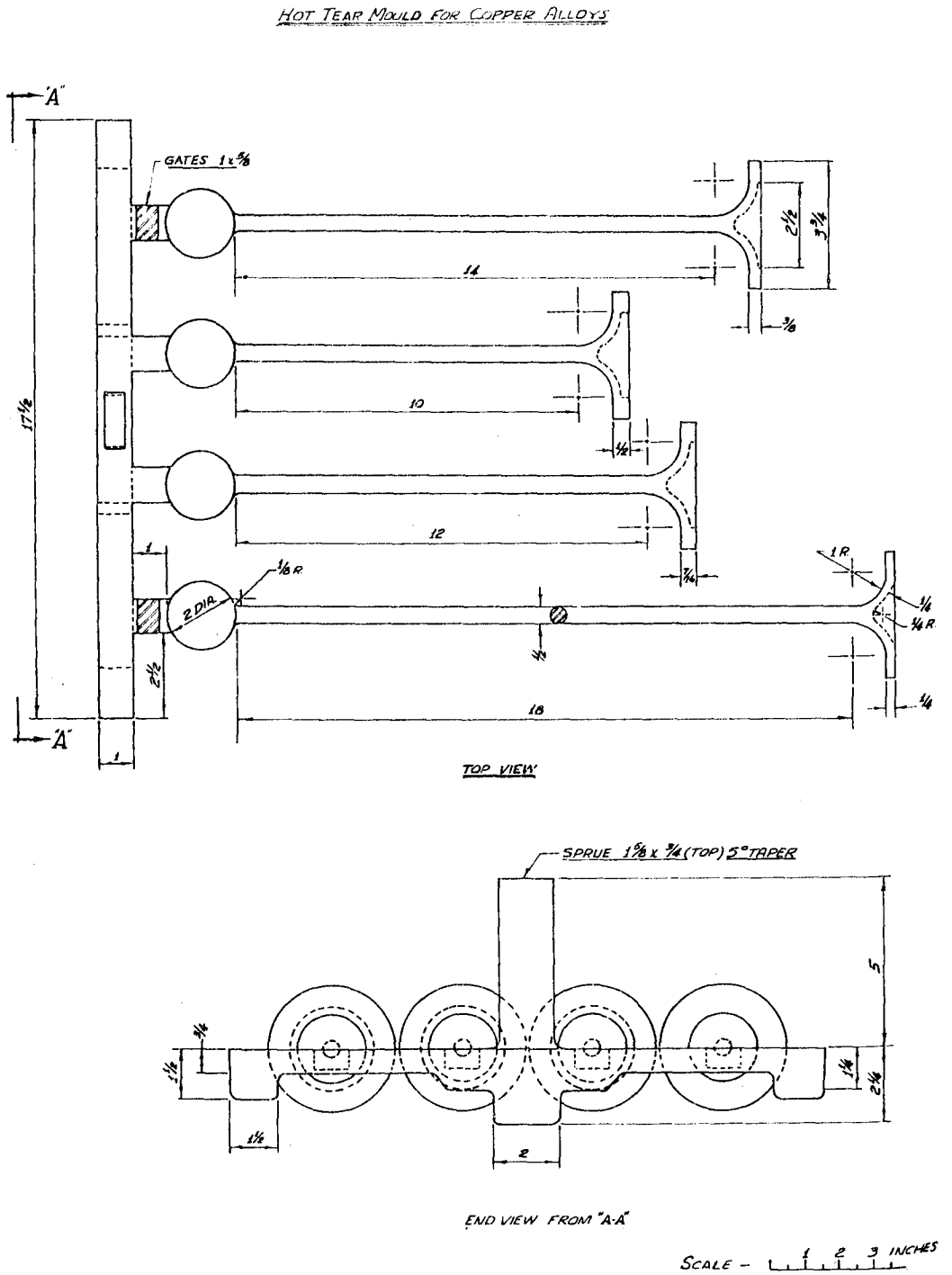


Figure 1 - Hot-tear Pattern.

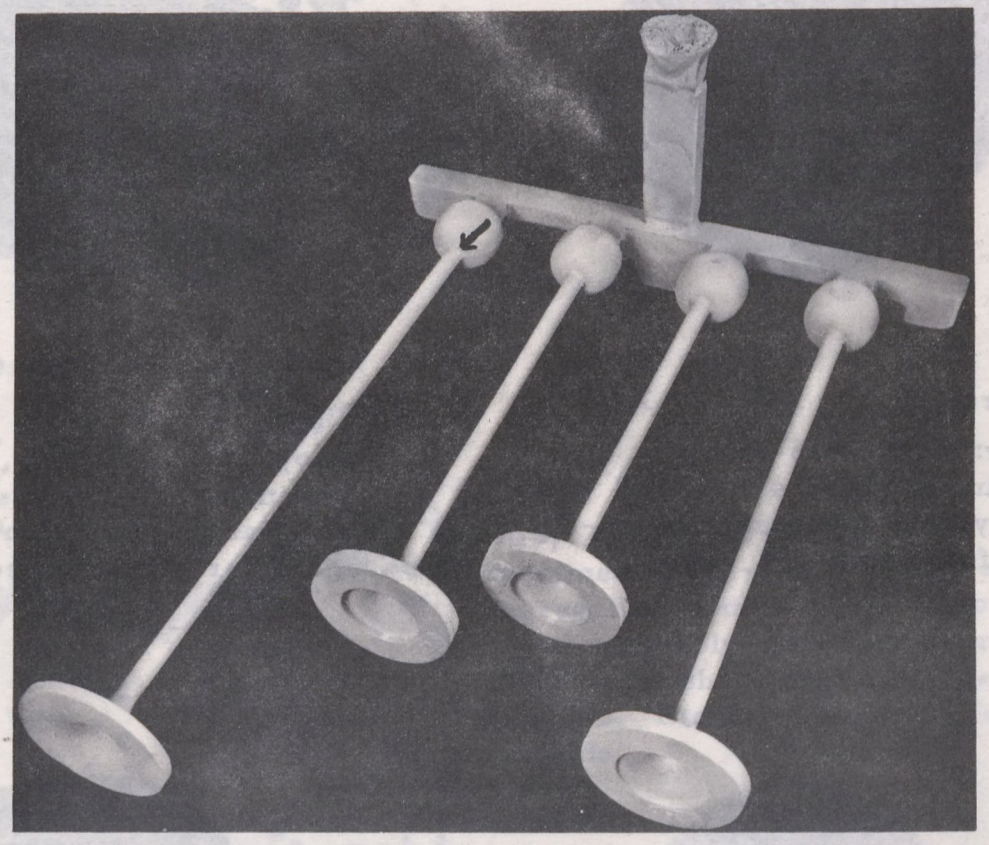

Figure 2 - Hot-tear Casting. Note crack at the ball-bar junction in 18-in. bar.

Figure 3 X3

Alloy: 4A (85-5-5-5)
Specimen: 826-2-4
Honeycomb appearance of hot-tear fracture.

Figure 4 X3

Alloy: 1A (88-10-0-2)
Specimen: 827-1-4
Hot-tear fracture with wide and differently oriented facets.

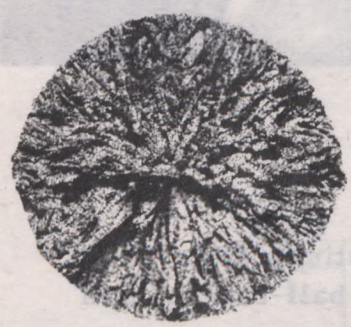

Figure 5 X3

Alloy: 4A (85-5-5-5)
Melt: 861
Hot tensile fracture - 800°C.

Figure 6 X3

Alloy: 1A (88-10-0-2)
Melt: 862
Hot tensile fracture - 800°C.

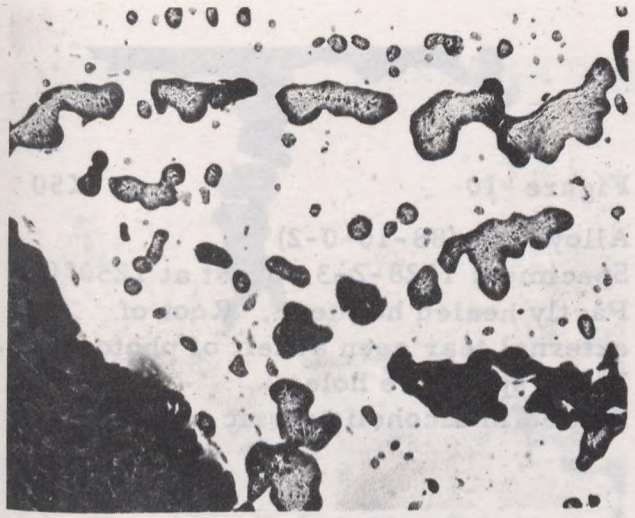

Figure 7 X100

Alloy: 3A (80-10-10)
Specimen: 1022-1-4. Cast at 1200°C.
Suggestion of lead globules alignment at the hot spot of the bar casting (top).
As polished.

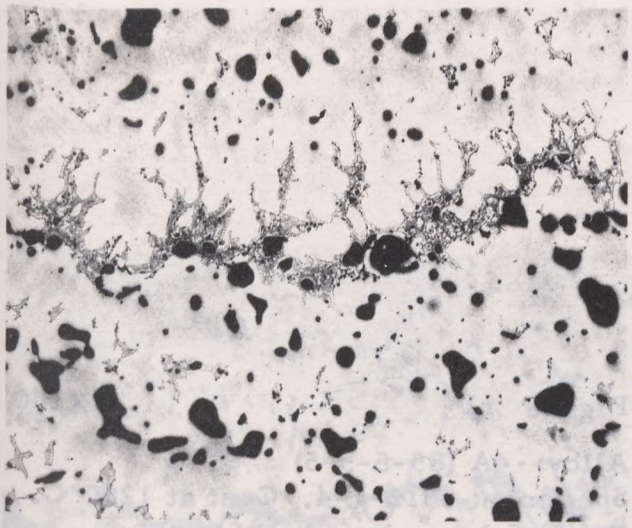

Figure 8 X100

Alloy: 3A (80-10-10)
Specimen: 1022-1-4. Cast at 1200°C
Segregation of delta phase at hot spot of bar; probably healed hot-tear.
Black spots show locations of lead globules. Etched in alcoholic ferric chloride.

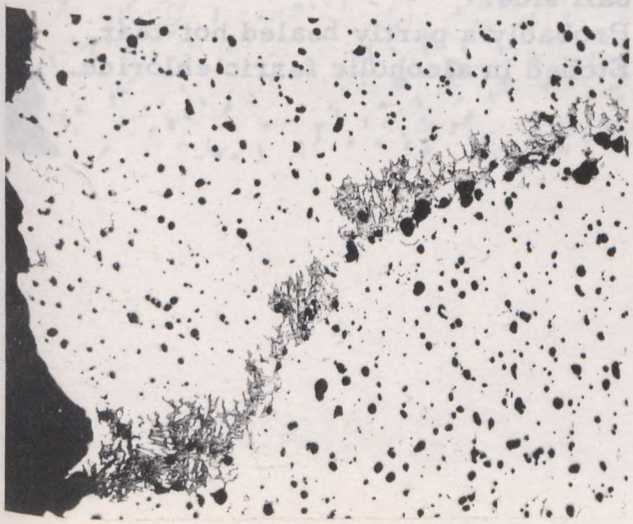

Figure 9 X100

Alloy: B.N.F. (87.5-7.5-3-2)
Specimen: 837-3-3. Cast at 1225°C.
Healed hot-tear at hot spot of casting (left of photograph).
Black spots are lead globules.
Etched in alcoholic ferric chloride.

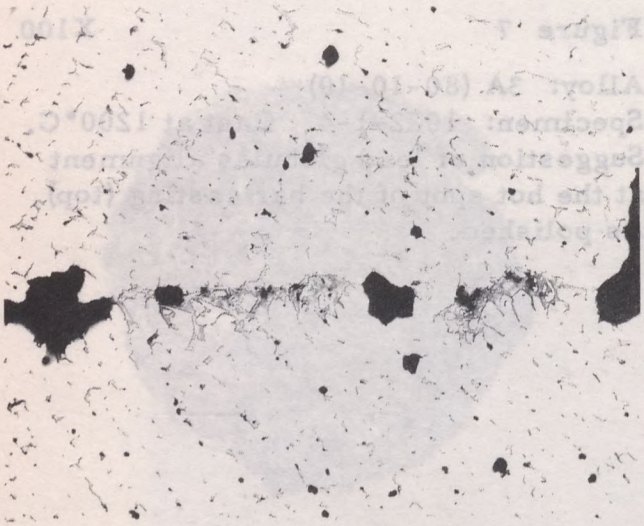

Figure 10 X50

Alloy: 1A (88-10-0-2)
Specimen: 1028-2-3. Cast at 1250°C.
Partly healed hot-tear. Root of external tear seen at left of photograph.
Black spots are holes.
Etched in alcoholic ferric chloride.

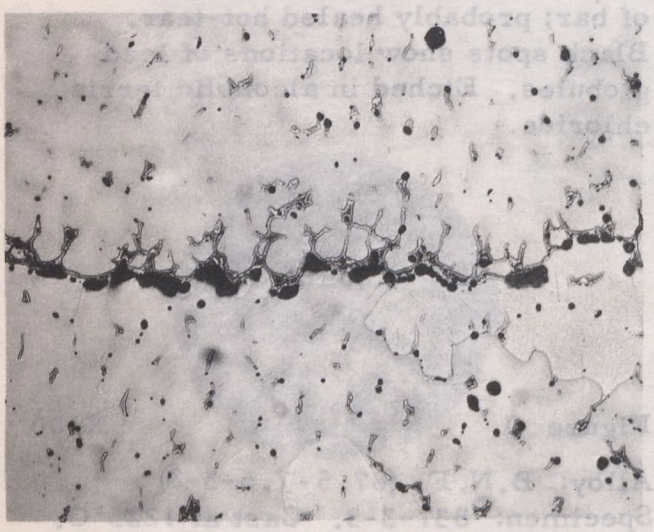

Figure 11 X100

Alloy: 4A (85-5-5-5)
Specimen: 1012-1-4. Cast at 1200°C.
Band of delta phase and holes in a direction normal to main axis of bar; ball side.
Probably a partly healed hot-tear.
Etched in alcoholic ferric chloride.

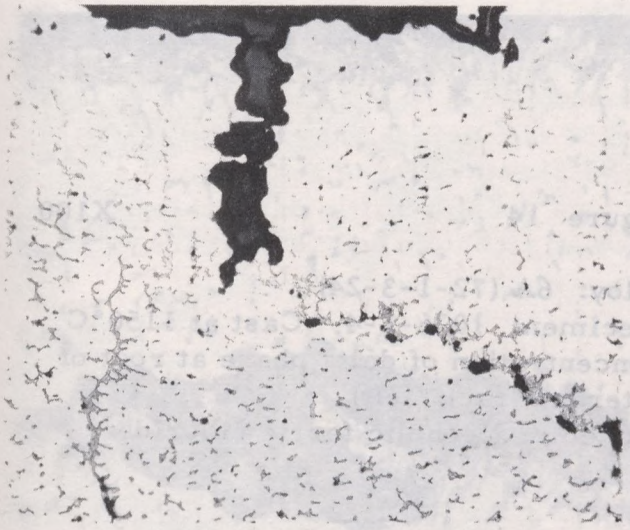

Figure 12 X40

Alloy: 1A (88-10-0-2)
Specimen: 819-1-3. Cast at 1275°C.
Heavy stringer of delta phase joining the root of an external hot-tear (top). Also a stringer of delta perpendicular to main axis of bar.
Etched in alcoholic ferric chloride.

Figure 13 X50

Alloy: 1A (88-10-0-2)
Specimen: 827-1-3. Cast at 1275°C.
Concentration of delta phase in line with an external hot-tear (left).
Partly healed hot-tear.
Etched in alcoholic ferric chloride.

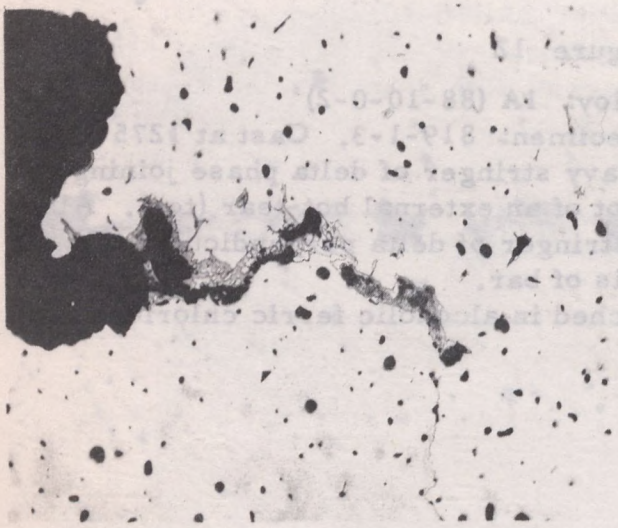

Figure 14 X100

Alloy: 6A (72-1-3-24)
Specimen: 1026-1-4. Cast at 1150°C.
Concentration of delta phase at root of external crack (left).
Etched in alcoholic ferric chloride.

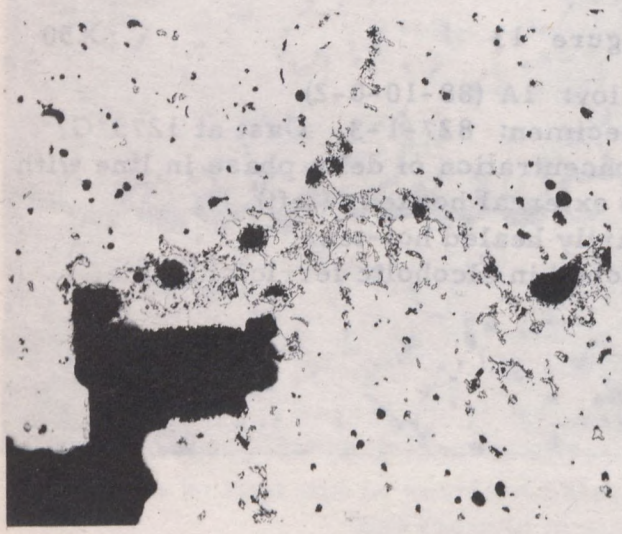

Figure 15 X100

Alloy: Inco (84.5-6.5-3.5-3.5-2)
Specimen: 817-1-3. Cast at 1275°C.
Concentration of delta phase at root of crack (left). Note that delta phase is more dispersed than in other alloys.
Etched in alcoholic ferric chloride.

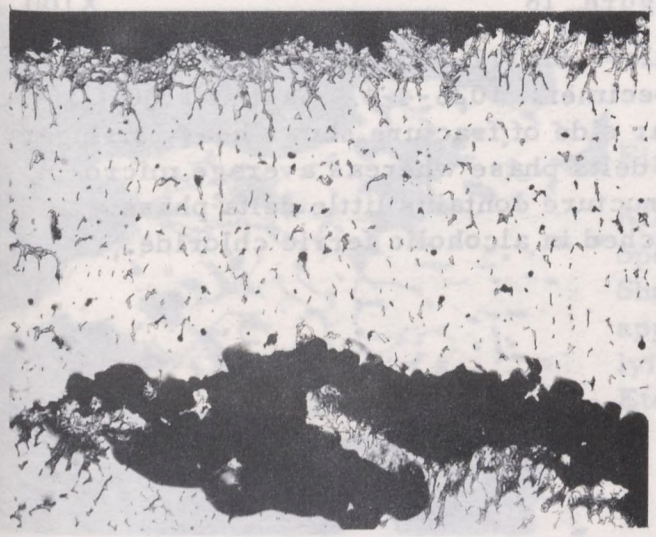

Figure 16 X50

Alloy: 1A (88-10-0-2)
Specimen: 1028-2-4. Cast at 1250°C.
Band of delta phase on bar side of fracture (top). A crack (bottom) is also lined with delta phase.
Etched in alcoholic ferric chloride.

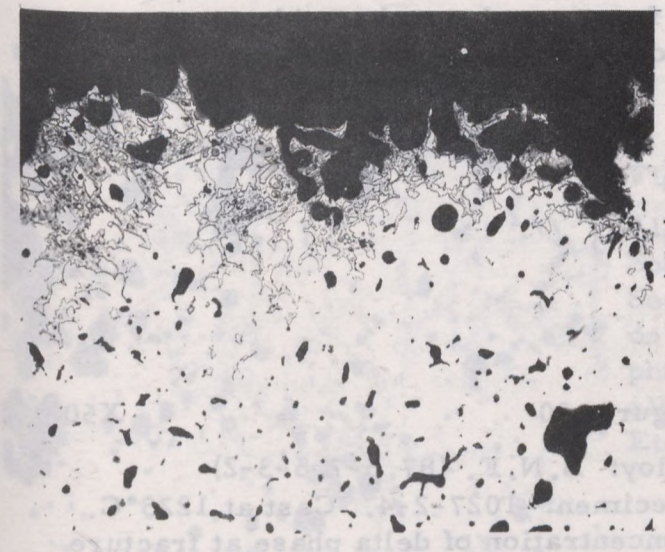

Figure 17 X100

Alloy: 5A (81-3-7-9)
Specimen: 863-1-4. Cast at 1275°C.
Very heavy concentration of delta phase on bar side of fracture (top). Black spots are holes or lead globules.

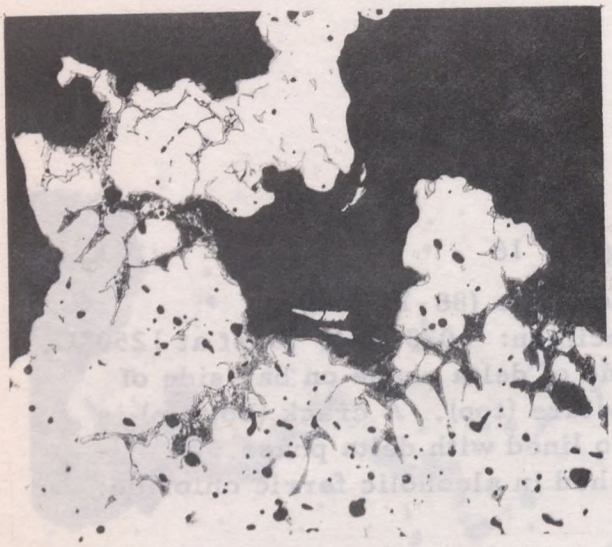

Figure 18 X100

Alloy: 6A (72-1-3-24)
Specimen: 1026-4-4. Cast at 1100°C.
Bar side of fracture shows heavy stringers of delta phase whereas average microstructure contains little delta phase.
Etched in alcoholic ferric chloride.

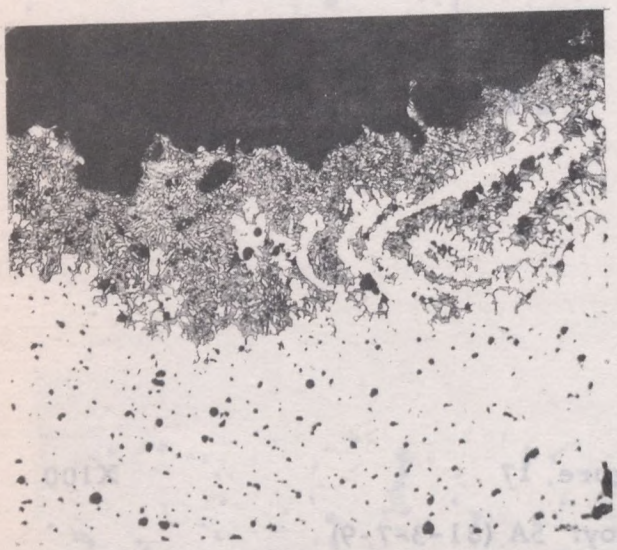

Figure 19 X50

Alloy: B.N.F. (87.5-7.5-3-2)
Specimen: 837-2-4. Cast at 1250°C.
Very heavy concentration of delta phase at fracture edge on bar side.
Etched in alcoholic ferric chloride.

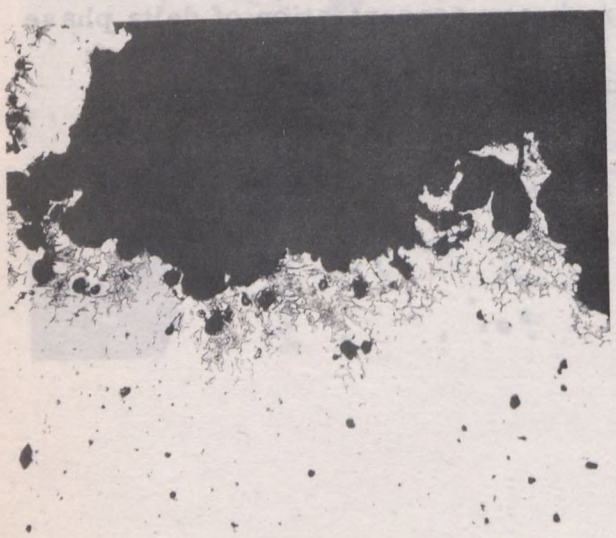

Figure 20 X50

Alloy: B.N.F. (87.5-7.5-3-2)
Specimen: 1027-2-4. Cast at 1225°C.
Concentration of delta phase at fracture edge on bar side.
Etched in alcoholic ferric chloride.

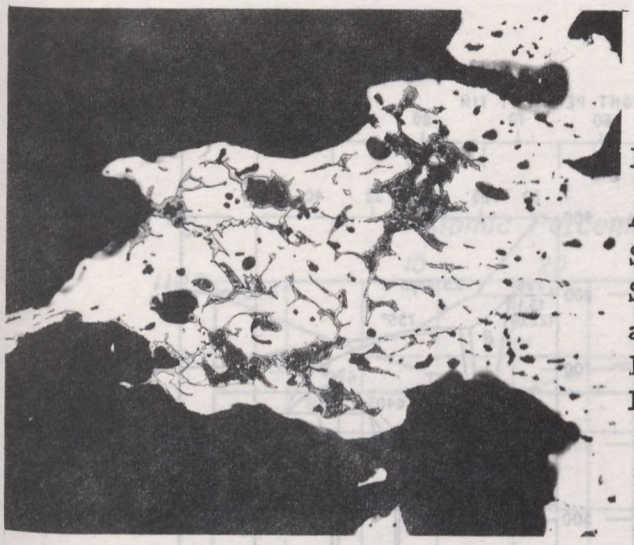

Figure 21 X100

Alloy: 6A (72-1-3-24)
Specimen: 1026-4-4. Cast at 1100°C.
Sharp peak in fracture section contains appreciably more delta phase than underlying material.
Etched in alcoholic ferric chloride.

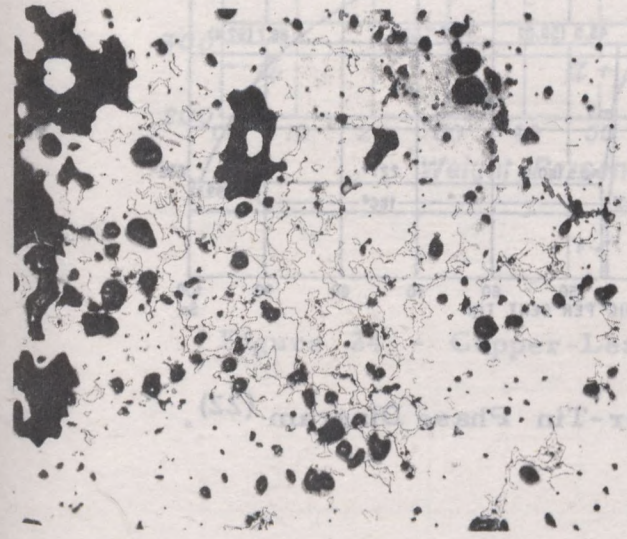

Figure 22 X100

Alloy: 4A (85-5-5-5)
Specimen: 1012-1-4. Cast at 1200°C.
Section through fracture of a bar mounted on end contains appreciably more delta phase than normal microstructure of alloy.
Etched in alcoholic chloride.

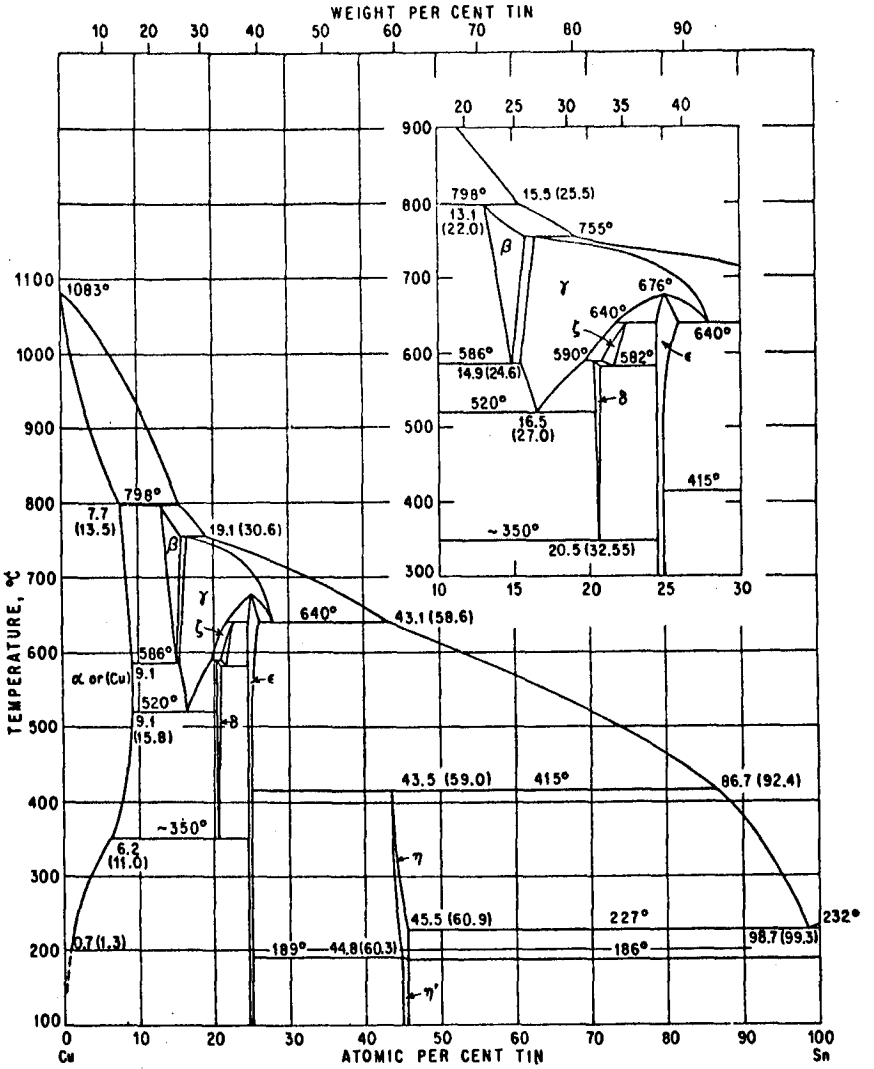


Figure 23 - Copper-Tin Phase Diagram [22].

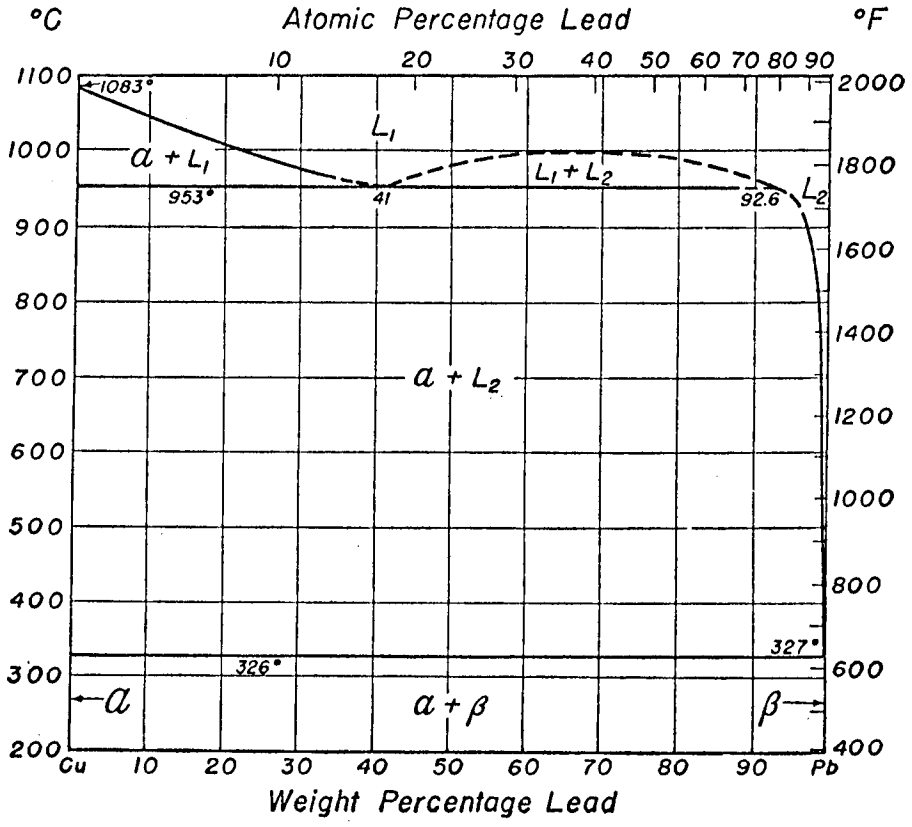


Figure 24 - Copper-Lead Phase Diagram [23].

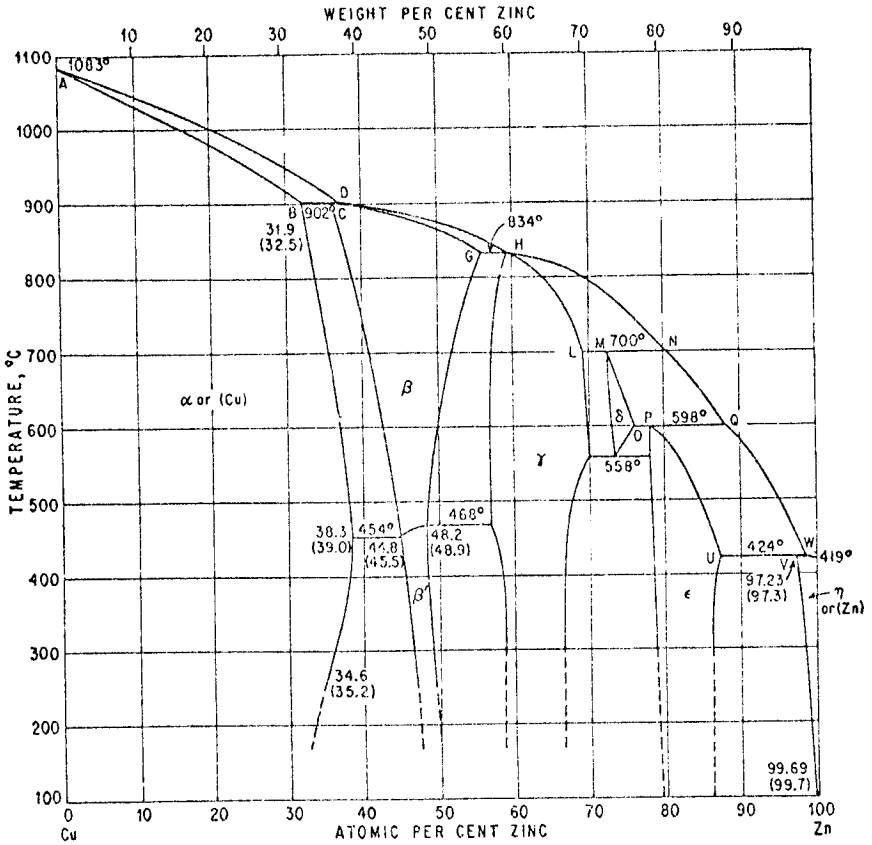


Figure 25 - Copper-Zinc Phase Diagram (22).

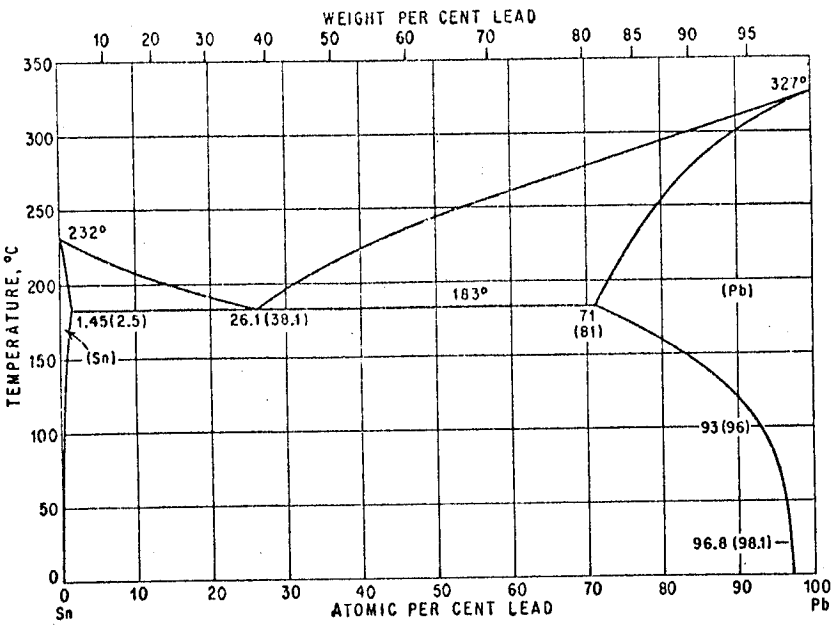


Figure 26 - Tin-Lead Phase Diagram (22).

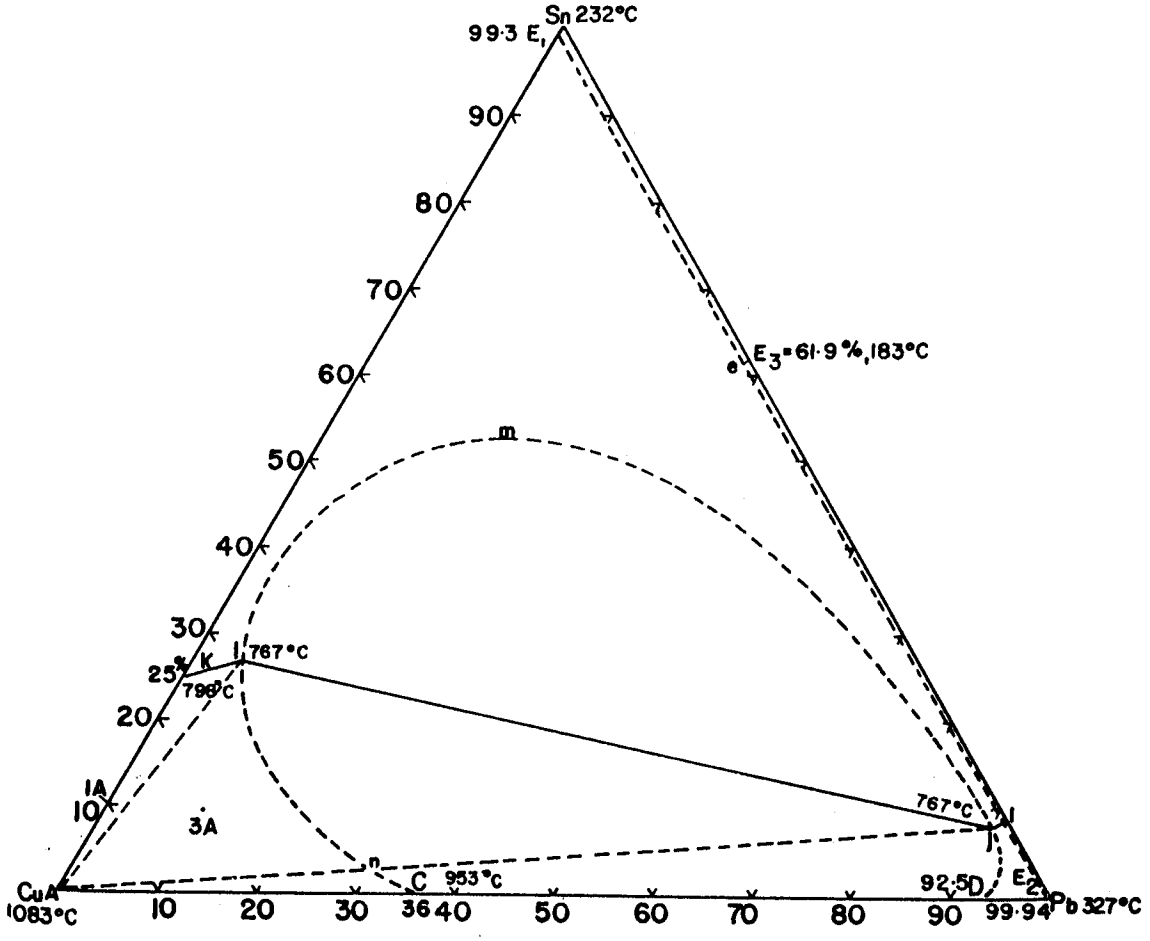


Figure 27 - Miscibility Gap in Copper-Tin-Lead System [24].

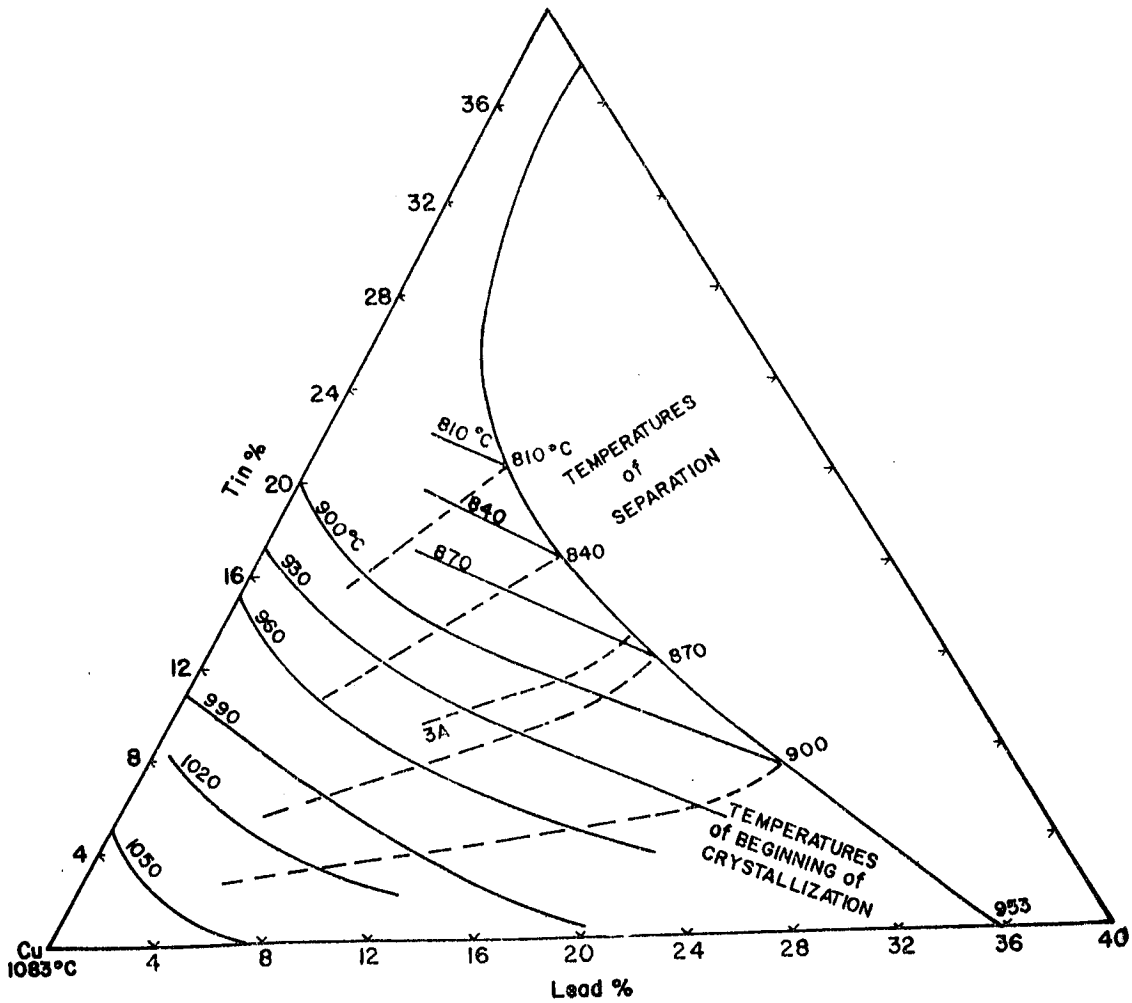


Figure 28 - Liquidus and Separation Surfaces in Copper-Tin-Lead System (25).

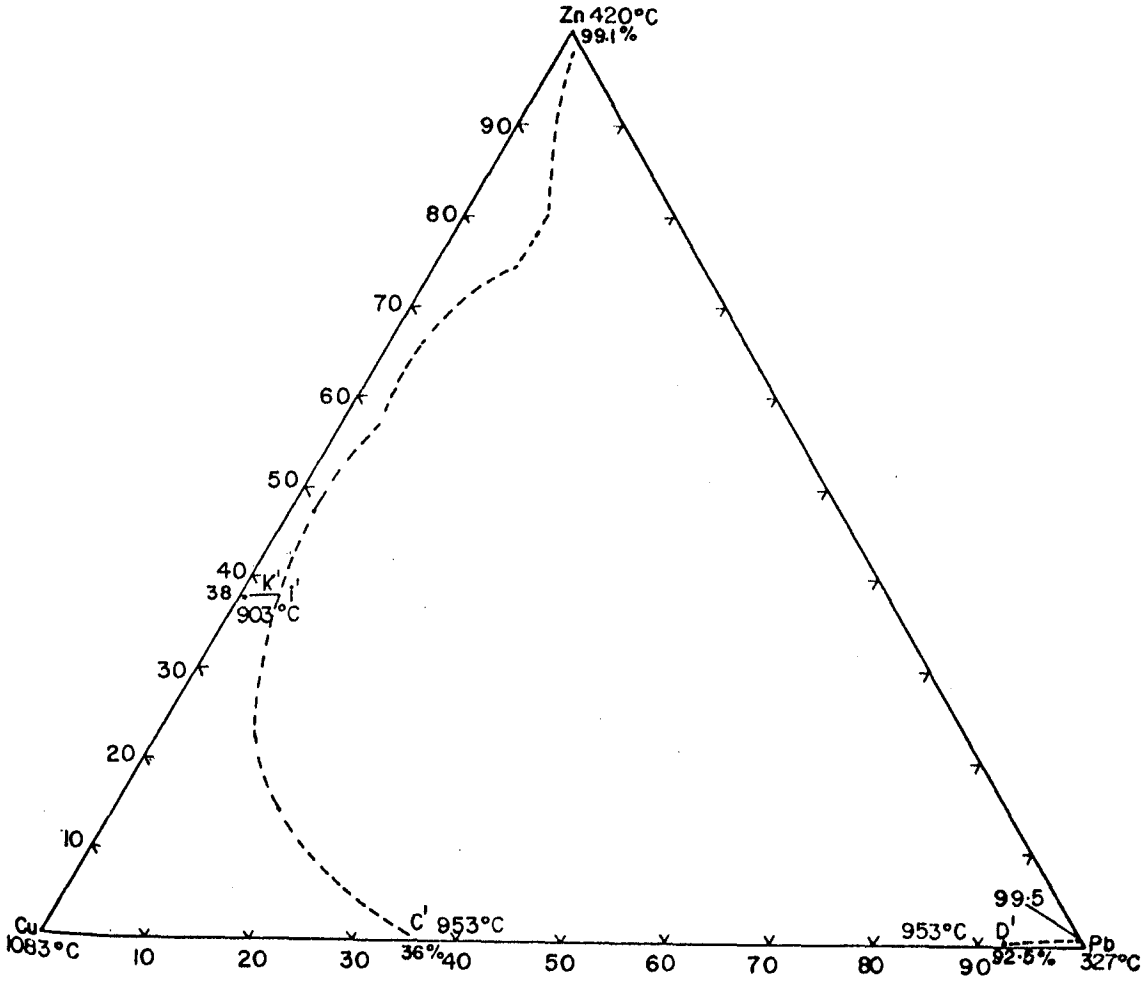


Figure 29 - Miscibility Gap in Copper-Zinc-Lead System [26].

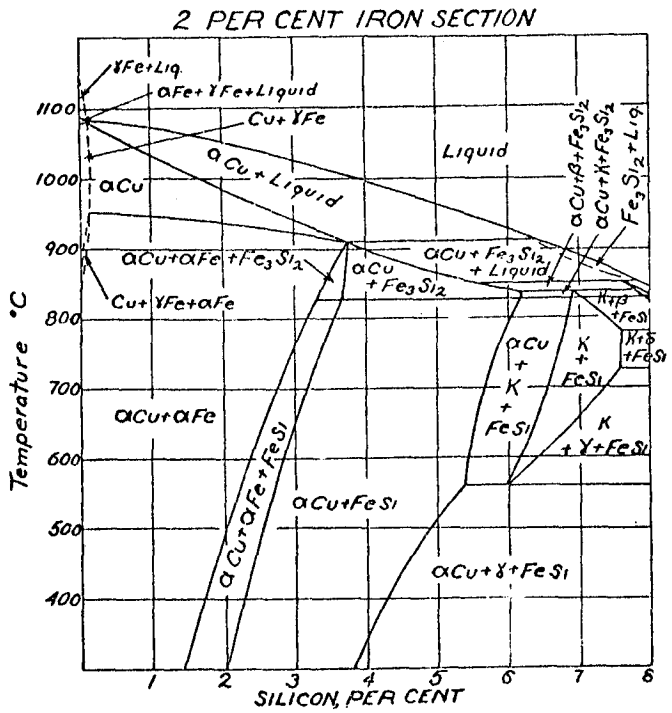


Figure 30 - Copper-Iron-Silicon Diagram, 2 wt % Iron Section (28).

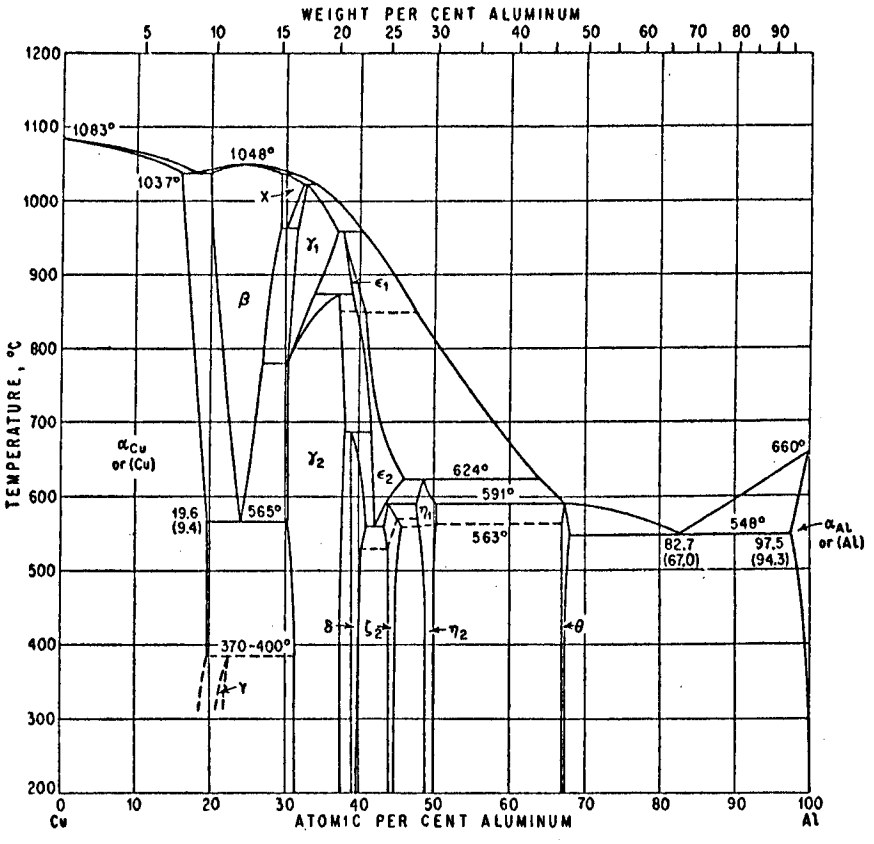


Figure 31 - Copper-Aluminum Phase Diagram [22].

TABLE 1

Chemical Composition [1]

| Alloy | Melt No[2] | Cu, % | Sn, % | Pb, % | Zn, % | P, % | Ni, % | Fe, % | Al, % | Mn, % | Si, % |
|---|---|---|---|---|---|---|---|---|---|---|---|
| | 819 | 87.43 | 9.77 | - | 2.44 | 0.028 | - | - | - | - | - |
| | 827 | 88.48 | 9.23 | - | 2.25 | 0.012 | - | - | - | - | - |
| | 869 | 87.97 | 9.81 | - | 1.99 | 0.015 | - | - | - | - | - |
| | 882 | 87.44 | 10.41 | - | 2.04 | 0.014 | - | - | - | - | - |
| 1A | 1006 | 88.31 | 9.46 | - | 1.96 | 0.003 | - | - | - | - | - |
| | 1011 | 87.34 | 9.55 | 0.15 | 2.69 | 0.015 | - | - | - | - | - |
| | 1017 | 87.72 | 10.43 | - | 1.63 | 0.010 | - | - | - | - | - |
| | 1036 | 87.15 | 10.17 | 0.49 | 2.07 | 0.019 | - | - | - | - | - |
| | 1039 | 87.88 | 9.94 | - | 2.34 | 0.039 | - | - | - | - | - |
| ASTM * | B143-52 | 86-89 | 9.0-11.0 | 0.30 | 1.0-3.0 | 0.05 | 1.0 | 0.15 | | | |
| | 1022 | 80.36 | 9.90 | 9.72 | - | 0.020 | - | - | - | - | - |
| 3A | 1035 | 81.87 | 9.15 | 9.12 | - | 0.004 | - | - | - | - | - |
| | B144-52 | 78-82 | 9.0-11.0 | 8.0-11.0 | 0.75 | 0.05 | 0.75 | 0.15 | | | |
| | 1007 | 85.18 | 4.58 | 4.94 | 4.71 | 0.003 | 0.14 | - | - | - | - |
| | 1012 | 84.76 | 5.93 | 4.85 | 4.15 | 0.011 | 0.25 | - | - | - | - |
| 4A | 1020 | 84.90 | 5.22 | 5.12 | 4.47 | 0.007 | - | - | - | - | - |
| | 1033 | 85.20 | 5.09 | 4.98 | 4.35 | 0.016 | 0.27 | - | - | - | - |
| ASTM | B145-52 | 84-86 | 4.0-6.0 | 4.0-6.0 | 4.0-6.0 | 0.05 | 1.0 | 0.30 | | | |
| | 1061 | 81.02 | 3.06 | 6.99 | 8.65 | 0.016 | - | - | - | - | - |
| 5A | 1068 | 80.72 | 3.58 | 6.99 | 8.12 | 0.014 | 0.16 | - | - | - | - |
| ASTM | B145-52 | 78-82 | 2.25-3.5 | 6.0-8.0 | 7.0-10.0 | 0.02 | 1.0 | 0.40 | | | |
| | 1026 | 72.42 | 1.75 | 2.64 | 23.04 | - | - | - | - | - | - |
| 6A | 1031 | 71.78 | 1.58 | 2.35 | 24.42 | - | - | - | - | - | - |
| | B146-52 | 70-74 | 0.75-2.0 | 1.5-3.75 | rem | - | - | 0.60 | | - | |
| | 1030 | 56.36 | 1.23 | 0.57 | 39.20 | - | - | 0.80 | 0.93 | 0.57 | - |
| 7A | 1067 | 60.16 | 0.89 | 0.75 | 35.93 | - | - | 0.92 | 0.90 | 0.55 | - |
| ASTM | B147-52 | 56-62 | 1.5 | 0.5-1.5 | rem | - | - | 2.0 | 1.5 | 1.5 | - |
| 8A | 1029 | 57.39 | - | - | 39.95 | - | - | 0.97 | 0.91 | 0.58 | - |
| ASTM | B147-52 | 55-60 | 1.0 | 0.40 | rem | - | 0.50 | 2.0 | 1.5 | 1.5 | - |
| | 818 | 88.21 | 0.21 | - | 5.99 | - | - | 1.90 | 0.05 | 0.18 | 3.25 |
| | 833 | 90.49 | 0.21 | - | 4.55 | - | - | 1.58 | 0.01 | 0.14 | 2.65 |
| | 870 | 91.30 | 0.21 | - | 3.92 | - | - | 1.62 | 0.07 | 0.08 | 2.78 |
| | 873 | 91.17 | 0.21 | - | 3.92 | - | - | 1.61 | 0.12 | 0.10 | 2.78 |
| 12A | 879 | 91.08 | 0.30 | - | 3.40 | - | - | 1.68 | 0.07 | 0.11 | 2.86 |
| | 1009 | 91.24 | 0.21 | - | 4.12 | - | - | 1.19 | - | 0.07 | 2.83 |
| | 1015 | 90.89 | 0.10 | - | 3.97 | - | - | 1.65 | - | 0.04 | 2.86 |
| | 1018 | 91.09 | 0.30 | - | 3.89 | - | - | 1.65 | - | - | 2.76 |
| ASTM | B198-52 | - | 1.0 | 0.50 | 5.0 | - | - | 2.5 | 1.5 | 1.5 | 1.0-5.0 |
| | 816 | 86.71 | 7.85 | 3.20 | 2.04 | 0.016 | - | - | - | - | - |
| | 837 | 86.88 | 7.46 | 3.42 | 2.02 | 0.020 | 0.16 | - | - | - | - |
| | 871 | 87.54 | 7.62 | 3.25 | 1.46 | 0.019 | 0.10 | - | - | - | - |
| | 884 | 87.57 | 7.48 | 3.29 | 1.50 | 0.003 | - | - | - | - | - |
| B.N.F. | 1008 | 86.37 | 6.72 | 3.85 | 2.56 | 0.001 | - | - | - | - | - |
| | 1013 | 87.17 | 8.39 | 2.90 | 1.51 | 0.016 | - | - | - | - | - |
| | 1021 | 87.71 | 7.51 | 2.90 | 1.74 | 0.010 | - | - | - | - | - |
| | 1038 | 87.52 | 7.69 | 2.95 | 1.85 | 0.011 | - | - | - | - | - |
| | Nominal | 87.5 | 7.5 | 3 | 2 | | | | | | |
| | 817 | 84.36 | 6.35 | 3.55 | 3.78 | 0.016 | 1.92 | - | - | - | - |
| | 848 | 85.44 | 6.28 | 3.42 | 2.82 | 0.026 | 2.00 | - | - | - | - |
| | 874 | 86.95 | 5.95 | 3.11 | 2.30 | 0.021 | 1.62 | - | - | - | - |
| | 889 | 85.50 | 6.07 | 3.54 | 2.53 | 0.009 | 1.94 | - | - | - | - |
| INCO | 1010 | 84.48 | 6.02 | 3.76 | 3.33 | 0.019 | 2.20 | - | - | - | - |
| | 1016 | 84.71 | 6.98 | 3.48 | 2.49 | 0.020 | 2.15 | - | - | - | - |
| | 1019 | 84.36 | 6.91 | 3.45 | 3.35 | 0.007 | 2.08 | - | - | - | - |
| | 1032 | 84.07 | 6.60 | 3.31 | 4.13 | 0.014 | 2.04 | - | - | - | - |
| | Nominal | 84.5 | 6.5 | 3.5 | 3.5 | - | 2 | - | - | - | - |
| | 1045 | 80.14 | 4.92 | 10.40 | 4.28 | 0.020 | - | - | - | - | - |
| Mod. 4A | 1047 | 81.08 | 4.95 | 9.67 | 3.87 | 0.021 | - | - | - | - | - |
| | 1054 | 80.03 | 5.43 | 9.91 | 4.58 | 0.016 | - | - | - | - | - |
| | Nominal | 80 | 5 | 10 | 5 | - | - | - | - | - | - |
| | 1138 | 89.44 | 10.69 | - | - | 0.005 | - | - | - | - | - |
| | 1139 | 90.24 | 9.48 | - | - | 0.015 | - | - | - | - | - |
| 89-11 | 1140 | 89.02 | 10.75 | - | - | 0.001 | - | - | - | - | - |
| | 1142 | 90.37 | 9.60 | - | - | 0.003 | - | - | - | - | - |
| | Nominal | 89 | 11 | - | - | - | - | - | - | - | - |
| Propeller | 1070 | 80.31 | - | - | - | - | 3.83 | 5.23 | 9.82 | 0.73 | - |
| Bronze | MIL-B-21230 | 78 min | - | 0.03 | - | - | 3-5.5 | 3 -5 | 8.5-11 | 3.5 | - |

(1) On the lines carrying specifications, single values are the maximum amounts permitted unless otherwise indicated.

(2) Melt numbers in the 800 series were used in the preliminary experiment; those in the 1000 and 1100 series were used in the main experiment.

* ASTM Standards were used because of the wide acceptance of the alloy nomenclature. Corresponding CSA specifications are to be found in CSA Standards HC, 3-1962. Copper Alloy Ingots for Remelting, and HC, 9-1962. Copper Alloy Sand Castings.

TABLE 2

Crack Rating in Preliminary Experiment
(6", 10", 14" and 18" Bars)

| Alloy Designation | Melt Number | Pouring Temperature 1275°C | 1250°C | 1225°C | 1200°C | Melt Total |
|---|---|---|---|---|---|---|
| 1A | 819 | 8 | 8 | 5 | 6 | 27 |
| | 827 | 6 | 6½ | 6 | 6½ | 25 |
| | 869 | 7½ | 7 | 7 | 7½ | 29 |
| | 882 | 6 | 7 | 7½ | 5½ | 26 |
| | Average* | 7 | 7 | 6½ | 6½ | 27 |
| Weighted Average** | | 10½ | 10½ | 10 | 10 | 41 |
| 12A | 818 | 11½ | 11 | 11 | 11½ | 45 |
| | 833 | 7 | 6 | 7½ | 7 | 27½ |
| | 870 | 7½ | 8 | 9 | 8 | 32½ |
| | 873 | 7½ | 7 | 8½ | 8 | 31 |
| | 879 | 8½ | 8 | 9½ | 11 | 37 |
| | Average | 8½ | 8 | 9 | 9 | 34½ |
| Weighted Average | | 13 | 12 | 13½ | 13½ | 52 |
| B.N.F. | 816 | 5½ | 6 | 7 | 6 | 24½ |
| | 837 | 4½ | 5 | 7 | 8 | 24½ |
| | 871 | 5½ | 6½ | 6 | 6½ | 24½ |
| | 884 | 7 | 6 | 6½ | 6½ | 26 |
| | Average | 5½ | 6 | 6½ | 7 | 25 |
| Weighted Average | | 8 | 9 | 10 | 10½ | 37½ |
| Inco | 817 | 6½ | 5½ | 8 | 6½ | 26½ |
| | 848 | 7 | 8 | 9 | 9 | 33 |
| | 874 | 7½ | 7½ | 7½ | 8 | 30½ |
| | 889 | 6 | 6 | 8 | 6 | 26 |
| | Average* | 7 | 7 | 8 | 7½ | 29 |
| Weighted Average | | 10½ | 10½ | 12 | 11 | 44 |

* Because average values have been rounded up (to the nearest ½), the total of those average values may differ slightly from the average calculated from the melt totals.

** The weighted averages are designed to make Tables 2 and 3 more comparable in that they are based on 6 moulds. They do not compensate for the different bar lengths, patterns and pouring temperatures.

TABLE 3

Crack Rating in Main Experiment
(10", 12", 14" and 18" Bars; 6 Moulds per Melt)

| Alloy Designation | Melt Number | Pouring Temperature | | | Melt Total |
|---|---|---|---|---|---|
| | | 1200°C | 1150°C | 1100°C | |
| 1A | 1006 | 13½ | 12½ | 10½ | 36½ |
| | 1011 | 15 | 12½ | 9½ | 37 |
| | 1017 | 11 | 9 | 10½ | 30½ |
| | 1036 | 17½ | 14 | 12½ | 44 |
| | 1039 | 15 | 14 | 11½ | 40½ |
| | Average* | 14½ | 12½ | 11 | 37½ |
| 3A | 1022 | 1½ | 5 | 2½ | 9 |
| | 1035 | 1 | 3½ | 3½ | 8 |
| | Average* | 1 | 4 | 3 | 8½ |
| 4A | 1007 | 19 | 16½ | 16 | 51½ |
| | 1012 | 20 | 19½ | 13½ | 53 |
| | 1020 | 23 | 20 | 20½ | 63½ |
| | 1033 | 20½ | 21 | 19 | 60½ |
| | Average* | 20½ | 19 | 17 | 57 |
| 5A | 1061 | 12 | 16-1/4 | 21½ | 49-3/4 |
| | 1068 | 10 | 19-3/4 | 19 | 48-3/4 |
| | Average | 11 | 18 | 20 | 49 |
| | ** | 1150°C | 1100° C | 1050°C | |
| 6A | 1026 | 19½ | 17 | 11½ | 48 |
| | 1031 | 16½ | 13 | 14½ | 44 |
| | Average | 18 | 15 | 13 | 46 |
| | ** | 1050°C | 1000°C | 960°C | |
| 7A | 1030 | 1 | 2 | 0 | 3 |
| | 1067 | 0 | 0 | 0 | 0 |
| 8A | 1029 | 0 | 0 | 0 | 0 |
| | | 1200°C | 1150°C | 1100°C | |
| 12A | 1009 | 23½ | 24½ | 22½ | 70½ |
| | 1015 | 23 | 25 | 24½ | 72½ |
| | 1018 | 26 | 26½ | 25 | 77½ |
| | Average | 24 | 25½ | 24 | 73½ |
| B.N.F. | 1008 | 16½ | 15 | 11½ | 43 |
| | 1013 | 14½ | 9½ | 8 | 32 |
| | 1021 | 17 | 15½ | 9½ | 42 |
| | 1038 | 13½ | 15½ | 14½ | 43½ |
| | Average | 15½ | 14 | 11 | 40½ |
| Inco | 1010 | 19½ | 18½ | 13 | 51 |
| | 1016 | 22½ | 20½ | 13½ | 56½ |
| | 1019 | 23 | 19½ | 15½ | 58 |
| | 1032 | 22½ | 22 | 20 | 64½ |
| | Average | 22 | 20 | 15½ | 57½ |
| 80-5-10-5 | 1045 | 8 | 17 | 10½ | 35½ |
| | 1047 | 8 | 16½ | 17 | 41½ |
| | 1054 | 12 | 17½ | 14 | 43½ |
| | Average* | 9½ | 17 | 14 | 40 |
| 89-11 | 1138 | 12 | 11½ | 7 | 30½ |
| | 1139 | 11 | 8 | 3½ | 22½ |
| | 1140 | 11 | 9 | 5 | 25 |
| | 1142 | 13 | 11½ | 4½ | 29 |
| | Average | 12 | 10 | 5 | 27 |
| Propeller Bronze | 1070 | 0 | 0 | 0 | 0 |

* Because average values have been rounded up (to the nearest ½), the total of those average values may differ slightly from the average calculated from the melt totals.

** Pouring temperatures reduced because of lower liquidus temperatures in these alloys.

TABLE 4

Influence of Pouring Temperature on Crack Rating
(Expressed as a Percentage of the Results for 4A Cast at 1200°C)

| Alloy Designation | Pouring Temperature *, °C | | |
|---|---|---|---|
| | 1200 | 1150 | 1100 |
| 1A | 72 | 60 | 53 |
| 3A | 6 | 21 | 15 |
| 4A | 100 | 93 | 83 |
| 5A | 54 | 88 | 98 |
| 6A* | 88 | 73 | 63 |
| 7A* | 2 | 5 | 0 |
| 8A* | 0 | 0 | 0 |
| 12A | 117 | 123 | 117 |
| B.N.F. | 75 | 67 | 53 |
| Inco | 107 | 98 | 75 |
| 80-5-10-5 | 45 | 83 | 67 |
| Propeller Bronze | 0 | 0 | 0 |
| 89-11 | 59 | 49 | 24 |

* Pouring temperatures were 1150°C, 1100°C and 1050° for 6A alloy, and 1050°C, 1000°C and 960°C for 7A and 8A alloys.

TABLE 5

Results of Differential Thermal Analysis

| Alloy | * Source | Chemical Composition, % | | | | | | | | | | "Thermal Arrests" at Cooling Rate of 10°C/min | | | | | Freezing Range,°C |
|---|---|---|---|---|---|---|---|---|---|---|---|---|---|---|---|---|---|
| | | Cu | Sn | Pb | Zn | P | Ni | Fe | Al | Mn | Si | A | B | C | D | E | |
| 1A | | 89.6 | 9.3 | - | 1.4 | - | - | - | - | - | - | 986 | - | - | 782 | - | 204 |
| | (5) | 88 | 10 | - | 2 | - | - | - | - | - | - | 1004 | - | - | 843 | - | 161 |
| 3A | | 80.8 | 9.5 | 9.5 | - | - | - | - | - | - | - | 950 | - | 866 | 767 | - | 183 |
| | (6) | 79 | 9.3 | 10.2 | 0.3 | 0.01 | 0.4 | 0.01 | - | - | - | 929 | - | - | 762 | 314 | 167 |
| 4A | | 84.7 | 4.9 | 4.9 | 4.4 | - | - | - | - | - | - | 1000 | 920 | 881 | 760 | 322 | 250 |
| | (6) | 85 | 4.4 | 5.1 | 4.6 | 0.01 | 0.7 | 0.1 | - | - | - | 1010 | - | - | 853 | 316 | 157 |
| 5A | | 81.4 | 3.0 | 6.5 | 8.6 | - | - | - | - | - | - | 987 | 911 | - | 760▽ | - | 227 |
| 6A | | 73.7 | 1.4 | 2.2 | 22.3 | - | - | - | - | - | - | 948 | 893 | - | 775 | - | 173 |
| | (7) | 75.8 | 2.7 | 5.6 | | - | 0.7 | 0.3 | - | - | - | 953 | - | - | 830 | 319 | 123 |
| 7A | | 61.5 | 1.2 | 1.2 | 32.8 | - | 0.1 | 1.1 | 1.0 | 0.5 | - | 890 | - | - | 860 | - | 30 |
| | (7) | 57.8 | 0.3 | 0.2 | 39.3 | - | 0.1 | 1.0 | 1.1 | 0.5 | - | 880 | - | - | 862 | - | 18 |
| 8A | | 61.47 | 0.3 | 0.71 | 33.58 | - | 0.08 | 1.15 | 1.05 | 0.63 | - | 890 | - | - | 860 | - | 30 |
| | (7) | 57.8 | 0.3 | 0.2 | 39.3 | - | 0.1 | 1.0 | 1.1 | 0.5 | - | 880 | - | - | 862 | - | 18 |
| 12A | | 91.29 | 0.21 | - | 2.42 | - | 0.06 | | | | | 1010 | - | - | 907 | - | 103 |
| B.N.F. | | 87.6 | 7.2 | 2.7 | 2.0 | - | - | - | - | - | - | 1000 | - | 842 | 761 | 322 | 239 |
| | (6) | 88 | 5.7 | 1.4 | 4.4 | 0.01 | 0.6 | 0.07 | - | - | - | 988 | - | - | 825 | - | 163 |
| Inco | | 85.5 | 6.4 | 3.8 | 2.5 | - | 2.0 | - | - | - | - | 1012 | 862 | 812 | 755 | 322 | 257 |
| 4A + Pb | | 80.2 | 5.3 | 9.6 | 4.3 | - | - | - | - | - | - | 972 | 900 | 860 | 755 | 319 | 217 |
| 89-11 | | 89.94 | 9.82 | - | - | - | - | - | - | - | - | 1005 | - | - | 794 | - | 211 |
| | (8) | 89 | 11 | - | - | - | - | - | - | - | - | 1000 | - | - | 831 | - | 169 |
| Prop. Br. | | 80.8 | - | - | - | - | 3.8 | 5.0 | 9.3 | 0.8 | - | 1053 | - | - | 1030 | - | 23 |
| | (8) | 81.5 | - | - | - | - | 5 | 2.5 | 9.5 | 1 | - | 1055 | - | - | 1035 | - | 20 |

* Source - Figures pertain to references. Most results were obtained upon heating at rates which are not given.

▽ Although no arrest was detected by thermal analysis, metallographic examination revealed the presence of small particles of $\delta$ which indicate that the effective solidus is in the vicinity of 760°C (1400°F).

A) First separation of Cu-rich $\alpha$.

B) Probable separation of lead-rich monotectic liquid in Cu-Pb-Sn system.

C) Separation of lead-rich monotectic liquid in Cu-Pb-Sn system.

D) Start of peritectic transformation in tin-rich alloys, and approximate "effective" solidus in all alloys.

E) Solidification of lead-rich phase.